



Review of Requirements and Status of Simulation and Scaling of Transonic, Viscous Flows

**J. Leith Potter
Registered Consulting Engineer
Nashville, Tennessee 37215**

September 1984

Final Report for Period August 24, 1983 — March 19, 1984

Approved for public release; distribution unlimited.

**ARNOLD ENGINEERING DEVELOPMENT CENTER
ARNOLD AIR FORCE STATION, TENNESSEE
AIR FORCE SYSTEMS COMMAND
UNITED STATES AIR FORCE**

NOTICES

When U. S. Government drawings, specifications, or other data are used for any purpose other than a definitely related Government procurement operation, the Government thereby incurs no responsibility nor any obligation whatsoever, and the fact that the government may have formulated, furnished, or in any way supplied the said drawings, specifications, or other data, is not to be regarded by implication or otherwise, or in any manner licensing the holder or any other person or corporation, or conveying any rights or permission to manufacture, use, or sell any patented invention that may in any way be related thereto.

Qualified users may obtain copies of this report from the Defense Technical Information Center.

References to named commercial products in this report are not to be considered in any sense as an endorsement of the product by the United States Air Force or the Government.

This final report was submitted by J. Leith Potter, Registered Consulting Engineer, Nashville, Tennessee, under contract F40600-83-C-0007 with the Arnold Engineering Development Center, Air Force Systems Command, Arnold Air Force Station, TN 37389. Dr. Keith L. Kushman was the AEDC Project Manager.

APPROVAL STATEMENT

This report has been reviewed and approved.



KEITH L. KUSHMAN
Directorate of Technology
Deputy for Operations

Approved for publication:

FOR THE COMMANDER



MARION L. LASTER
Director of Technology
Deputy for Operations

UNCLASSIFIED

SECURITY CLASSIFICATION OF THIS PAGE

REPORT DOCUMENTATION PAGE

1a. REPORT SECURITY CLASSIFICATION UNCLASSIFIED			1d. RESTRICTIVE MARKINGS		
2a. SECURITY CLASSIFICATION AUTHORITY			3. DISTRIBUTION/AVAILABILITY OF REPORT Available for Public Release; Distribution is Unlimited.		
2b. DECLASSIFICATION/DOWNGRADING SCHEDULE			5. MONITORING ORGANIZATION REPORT NUMBER(S)		
4. PERFORMING ORGANIZATION REPORT NUMBER(S) AEDC-TR-84-23			7a. NAME OF MONITORING ORGANIZATION		
6a. NAME OF PERFORMING ORGANIZATION J. Leith Potter, Registered Consulting Engineer		6b. OFFICE SYMBOL (If applicable) DOT	7b. ADDRESS (City, State and ZIP Code)		
6c. ADDRESS (City, State and ZIP Code) 200 Sheffield Place Nashville, Tennessee 37215			8a. NAME OF FUNDING/SPONSORING ORGANIZATION Arnold Engineer- ing Development Center		
8b. OFFICE SYMBOL (If applicable) DO			9. PROCUREMENT INSTRUMENT IDENTIFICATION NUMBER		
8c. ADDRESS (City, State and ZIP Code) Air Force Systems Command Arnold Air Force Station, TN 37389			10. SOURCE OF FUNDING NOS		
11. TITLE (Include Security Classification) See Reverse of This Page			PROGRAM ELEMENT NO. 65807F	PROJECT NO.	TASK NO.
12. PERSONAL AUTHOR(S) Potter, J. Leith, Registered Consulting Engineer			WORK UNIT NO.	15. PAGE COUNT 62	
13a. TYPE OF REPORT Final Report			13b. TIME COVERED FROM 8/24/84 TO 3/19/84		14. DATE OF REPORT (Yr., Mo., Day) September 1984
16. SUPPLEMENTARY NOTATION Available in Defense Technical Information Center (DTIC).					
17. COSATI CODES			18. SUBJECT TERMS (Continue on reverse if necessary and identify by block number)		
FIELD	GROUP	SUB GR	Reynolds number		
20	04		boundary layer transition		
14	02		swept wings vortex separation (Cont)		
19. ABSTRACT (Continue on reverse if necessary and identify by block number) The elements of transonic, viscous-flow simulation are reviewed, documented, and briefly evaluated in the light of newer results from research in this field. Not only the case of wing flows at low angles of attack, but also the problems arising with wings and fuselages or missiles at higher angles are discussed. Criteria to be satisfied in scale-model testing and means for doing that are the principal topics covered. This includes the experimental techniques for simulating shock wave-boundary layer interaction, obtaining full-scale shock location and overall aerodynamic coefficients, and the precautions associated with boundary layer tripping in various types of testing. Vortical flows receive attention, and the requirement for assessing Reynolds number effects is emphasized. The review brings together information from diverse sources that wind tunnel test planners need in further improving experimental results and which is also critical in extrapolating those data to full-scale flight conditions. The subject of this report will continue to be of concern even though capabilities in (Cont)					
20. DISTRIBUTION/AVAILABILITY OF ABSTRACT UNCLASSIFIED/UNLIMITED <input type="checkbox"/> SAME AS RPT <input checked="" type="checkbox"/> DTIC USERS <input type="checkbox"/>			21. ABSTRACT SECURITY CLASSIFICATION UNCLASSIFIED		
22a. NAME OF RESPONSIBLE INDIVIDUAL W.O. Cole			22b. TELEPHONE NUMBER (Include Area Code) (615)455-2611 ext.7813		22c. OFFICE SYMBOL DOS

UNCLASSIFIED

SECURITY CLASSIFICATION OF THIS PAGE

11. TITLE

Review of Requirements and Status of Simulation and Scaling of Transonic, Viscous Flows

18. SUBJECT TERMS (Cont)

free-stream turbulence
vortical flows
scale-model testing

shock wave-boundary layer interaction
boundary layer tripping

19. ABSTRACT (Cont)

computational fluid dynamics are rapidly growing, and the recently dedicated National Transonic Facility (NTF) at the Langley Research Center will provide much increased test Reynolds numbers.

UNCLASSIFIED

SECURITY CLASSIFICATION OF THIS PAGE

PREFACE

The work reported herein was conducted by Dr. J. Leith Potter under contract F40600-83-C-0007 for the Directorate of Technology, Arnold Engineering Development Center (AEDC), Air Force Systems Command, Arnold Air Force Station, Tennessee. The AEDC Project Manager was Dr. Keith L. Kushman, AEDC/DOT. This report covers work on this contract for the period August 24, 1983 through March 19, 1984, and the manuscript was submitted for publication on June 15, 1984.

CONTENTS

	<u>Page</u>
1.0 INTRODUCTION	7
2.0 FLOW CONSIDERATIONS	8
2.1 Shock Wave-Boundary Layer (SBL) Interaction	8
2.2 The Case of Swept Wings	14
2.3 The Unit Reynolds Number	15
2.4 Locating the Terminal Shock Wave	18
2.5 Vortex Separation	20
3.0 SIMULATION REQUIREMENTS	28
4.0 INFLUENCING BOUNDARY LAYERS TO SIMULATE HIGHER REYNOLDS NUMBERS	31
4.1 Boundary Layer Transition and Thickness	31
4.2 Vortex Generators	39
4.3 Free-Stream Turbulence	41
5.0 WIND TUNNEL TESTING PRACTICES	42
5.1 Scaling for Aerodynamic Coefficients	44
6.0 CONCLUDING REMARKS	48
REFERENCES	50

ILLUSTRATIONS

<u>Figure</u>	<u>Page</u>
1. Transonic Flow Over an Airfoil at Various Mach Numbers for a 2-deg Angle of Attack. From Chang (Ref. 1)	10
2. Some Details (Schematic) of the Region of Interaction Between Turbulent Boundary Layer and Shock Wave. From Pearcey et al. (Ref. 2)	11
3. Flow Models for the Initial Development of Shock-Induced Separation (Schematic); Turbulent Boundary Layers (Successive Stages in a Mach Number or Incidence Increase). From Pearcey et al. (Ref. 2)	12
4. Flow-Model B in the Particular Form Under Consideration. From Osborne and Pearcey (Ref. 3)	13
5. Influence of Reynolds Number on the Properties of Shock-Induced Separation at Mach 1.5 (Conjectural). From Green (Ref. 7)	14
6. Basic Shock Pattern. From Hall (Ref. 10)	15
7. Surface Flow Beneath Swept Shocks. From Green (Ref. 5)	16

<u>Figure</u>	<u>Page</u>
8. Separation Beneath Swept Shocks. From Green (Ref. 5)	17
9. Flow Pattern for Swept, Short Bubble and Trailing-Edge Separation. From Hall (Ref. 10)	18
10. Flow Pattern for Vortex Separation. From Hall (Ref. 10)	18
11. Trailing-Edge Pressure Coefficient as a Function of Correlation Parameter K. From Khan and Cahill (Ref. 15)	20
12. Leading-Edge Separation Boundaries on Plane and Cambered Wing of Aspect Ratio 4/3. From Squire (Ref. 18)	22
13. Effect of Reynolds Number on Vortex-Flow Development — F-111 TACT Flight Experiment; $\alpha = 6$ deg, $M_\infty = 0.6$. From Polhamus and Gloss (Ref. 22)	23
14. Classical Leading-Edge Vortex Characteristics. From Miller and Wood (Ref. 23)	23
15. Variation of Lift Coefficient with Reynolds Number Where Leading-Edge Separation and Vortical Flow Exist. From Waggoner (Ref. 24)	25
16. Effect of Reynolds Number on Side-Force Coefficient for an Ogive- Cylinder Body of Revolution. From Jorgensen (Ref. 26), Credited to Keener (Ref. 25)	26
17. Wind Tunnels and Flight Reynolds Numbers	30
18. Distribution of Boundary Layer Parameters Downstream of 0.066-in.- diam Roughness Elements at $x_k = 2$ ft. From Klebanoff and Tidstrom (Ref. 35)	34
19. Variation of the Normalized Free-Stream Transition Reynolds Number with Sweep at Subsonic Mach Number. From Jillie and Hopkins (Ref. 49)	37
20. Variation of the Normalized Free-Stream Transition Reynolds Number with Sweep at Supersonic Mach Number. From Jillie and Hopkins (Ref. 49)	38
21. Effect of Vortex Generators on Shock Location and Pressure Recovery. From Cahill (Ref. 51)	40
22. Variation of Shock Location with Reynolds Number. From Baals (Ref. 61)	47
23. Idealized Graphical Trend of Data with Transition Location	47

TABLES

<u>Table</u>	<u>Page</u>
1. Data on Supersonic Boundary Layer Downstream of 3-D Trips. From Peterson (Ref. 34)	32
2. Example Trip-Size Estimates. (Method of Ref. 45)	36
NOMENCLATURE	56

1.0 INTRODUCTION

The basic approach of experimental aerodynamics is to strive for dynamic similarity in (usually) subscale laboratory apparatus and extend the measured data to full-scale, free-flight conditions by means of applicable scaling laws. Unfortunately, practical obstacles sometimes prevent the fulfillment of similarity conditions, and this is a matter of continuing concern. The two principal fluid dynamic scaling parameters in this work are the Reynolds and Mach numbers, and it has proved easier to duplicate flight Mach numbers than Reynolds numbers. For most current, manned aircraft, it is typical procedure to test an aerodynamic model, with its major features faithfully scaled in proportion to its full-sized counterpart, in a wind tunnel at Mach numbers equal to those expected in full-scale operation, but at Reynolds numbers appreciably less than the flight values. Thus, one must not only determine what similarity requirements should be satisfied, but also how to scale the laboratory results to compensate for the deficiencies in dynamic simulation.

Geometric scaling of major features generally does not include details such as structural joints and fasteners. A possibly more serious deficiency in similarity is the usual absence of a propulsion system when aerodynamic models are tested. However, these are not the subjects of this discussion.

The specific problem dealt with in this report is the simulation and scaling of transonic, viscous flows when models of aircraft and missiles or their components are tested in wind tunnels which do not enable data to be obtained at Reynolds numbers equal to those that will be attained in full-scale free flight. This statement should not be taken to imply that the duplication of full-scale Reynolds numbers is the only requirement for adequate simulation. In addition to the Mach number, it is well known that other conditions have to be satisfied. Wind tunnel experimenters must be concerned with accuracy in model dimensions, support-system interference, model deflections under load, free-stream flow angularity, turbulence, flow blockage, and effects that may arise from failure to duplicate the unit Reynolds number and wall-to-ambient-temperature ratio. However, it is the deficiency in Reynolds numbers and associated effects that are under scrutiny here.

The state-of-the-art of viscous, transonic-flow simulation and scaling is reviewed and the possibilities for improvement in testing techniques are considered. Prior studies have revealed that this is a very complex problem, especially when three-dimensional (3-D) flows must be dealt with. Therefore, it seems best to briefly review the background and summarize the requirements for satisfactory simulation as the starting point before discussing what may be done in seeking improvements. Knowing that the problem is severe, one must aim for the establishment of a hierarchy of requirements so that compromises may be identified.

2.0 FLOW CONSIDERATIONS

2.1 SHOCK WAVE-BOUNDARY LAYER (SBL) INTERACTION

One of the characteristics of transonic flow is the interaction between shock waves and boundary layers. Simulating and scaling so that wind tunnel tests will lead to correct predictions of aircraft performance and loads requires that SBL interaction be essentially the same on the scale model and the full-scale aircraft. Failure to match flight Reynolds numbers causes boundary layer characteristics to be different on the model tested. Skin friction, boundary layer separation, and interaction of the boundary layer with shock waves are influenced by the laminar or turbulent character of the boundary layer and also by its thickness and details of its structure. For a given body shape, attitude, wall-to-ambient-temperature ratio, and Mach number, these qualities depend on Reynolds number. (Uniformity and steadiness of free-stream flow, as well as freedom from wall interference and other such factors, is assumed in this discussion but should not be overlooked in specific cases.) In regard to transonic flows, most attention has focused on boundary layer separation related to shock wave interaction, particularly on airfoils or wings. This is because shock location and extent of separation are very important in determining pressure distributions on wings. Other regions of transonic aircraft may also be sites of SBL interaction. Examples are air intakes, deflected control surfaces, and internal flows at off-design conditions such as may occur in exhaust nozzles. However, flow over wings is the principal concern, so that is the focus of most of this discussion.

A number of very informative papers on this subject have appeared in AGARD (Advisory Group for Aerospace Research and Development) conference proceedings which will be referred to later. Much of the subsequent discussion will be based on the flow features sketched in Figs. 1, 2, 3, and 4. The first figure, taken from Chang (Ref. 1) shows the sequence of shock wave development in transonic flows over an airfoil at low angle of attack. The following features are illustrated:

1. At $M_\infty = 0.75$ — only a small region of locally supersonic flow exists in this particular example, and no shock wave forms. The wake separates near the trailing edge. (More thorough discussion of separation follows in the next paragraph.)
2. At $M_\infty = 0.81$ — a compression shock is seen on the upper surface, and the effect is apparent in the velocity distribution. Downstream of the shock, the flow continues subsonically to the trailing edge, and separation occurs. It should be noted that lambda shocks may be formed, usually being associated with laminar boundary layers and separation at the shocks. Typically,

multiple lambda shocks merge into a single lambda shock as Mach number increases. When the Reynolds number is increased and the boundary layer becomes turbulent, the oblique leg of the lambda shock disappears, leaving a near-normal shock as shown in Fig. 1.

3. At $M_\infty = 0.89$ — a more extensive area of supersonic flow exists, and the upper-surface shock is located farther aft. A lower-surface shock is located near the trailing edge.
4. At $M_\infty = 0.98$ and 1.4 — on both upper and lower surfaces the local flow is mainly supersonic.

When the strength of the shock increases enough to cause the boundary layer to separate, the extent of separation can be sufficient to influence the pressure at the trailing edge. This affects the airfoil circulation, its pressure distribution, and its overall performance. Pearcey et al. (Ref. 2), have described this situation in detail. Figures 2 and 3 are reproduced from their paper to make later references to their work easier.

Pearcey et al. distinguished between two flow models, A and B. The former identifies an SBL interaction wherein the only separation occurs at the foot of the shock wave and the separation bubble grows from the shock toward the trailing edge as shock strength increases (see Fig. 2a). Model B flow is that wherein separation is incipient or actually present at the trailing edge (see Fig. 2b). If the separation bubble of a Model A flow grows rearward all of the way to the trailing edge, it becomes a form of Model B flow. Model B includes other combinations of shocks and separation, but it always is characterized by trailing-edge separation (see Fig. 3). The boundary layer is assumed to be turbulent, and flow over airfoils and wings is considered in the discussion of these flow models in Ref. 2.

According to Pearcey et al., Model A flows are better simulated in wind tunnel testing because bubble growth spreading from the foot of the shock is not particularly sensitive to thickness or profile of the boundary layer, provided that it is turbulent at separation.

Osborne and Pearcey (Ref. 3) later described another variant of flow Model B. This case is one in which a small region of supersonic flow near the leading edge induces a shock which appreciably modifies development of rear separation. Figure 4, taken from Ref. 3, illustrates this phenomenon which may arise when free-stream Mach number is relatively low, but angle of attack is high. The influence of transition fixing when dealing with this type of flow was discussed in the referenced paper, but no easy testing procedure was recommended.

It should be noted that most published data and discussions pertain to the type of airfoils for which upper-surface flow receives most attention. The focus on the upper surface is also

apparent in this report, but it is obvious that the same considerations may apply to lower surfaces when shocks and separations become important there. For example, supercritical airfoil lower surfaces in some circumstances deserve the level of attention previously devoted only to upper surfaces of older airfoil designs. An informative discussion of flow over supercritical airfoils and wings has been presented by Yoshihara and Zonars (Ref. 4).

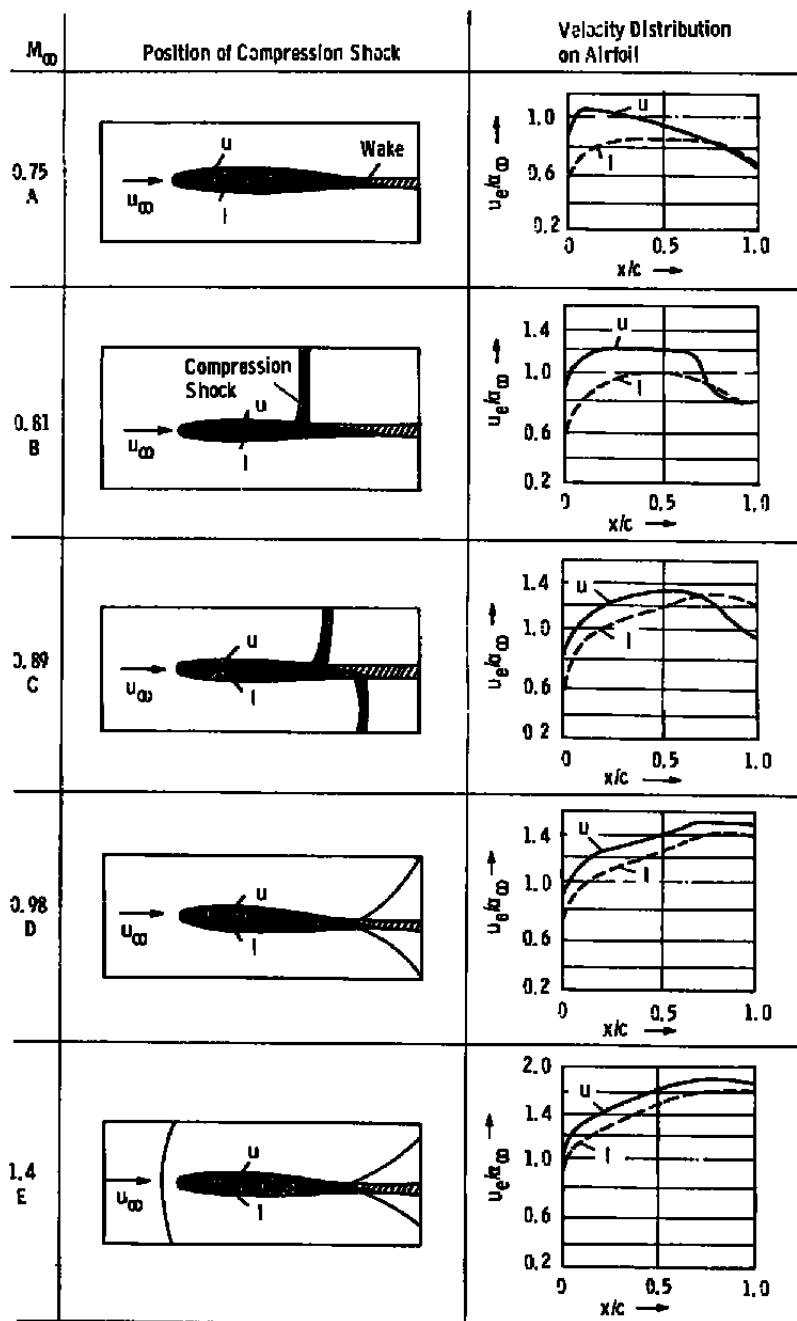


Figure 1. Transonic flow over an airfoil at various Mach numbers for a 2-deg angle of attack. From Chang (Ref. 1)

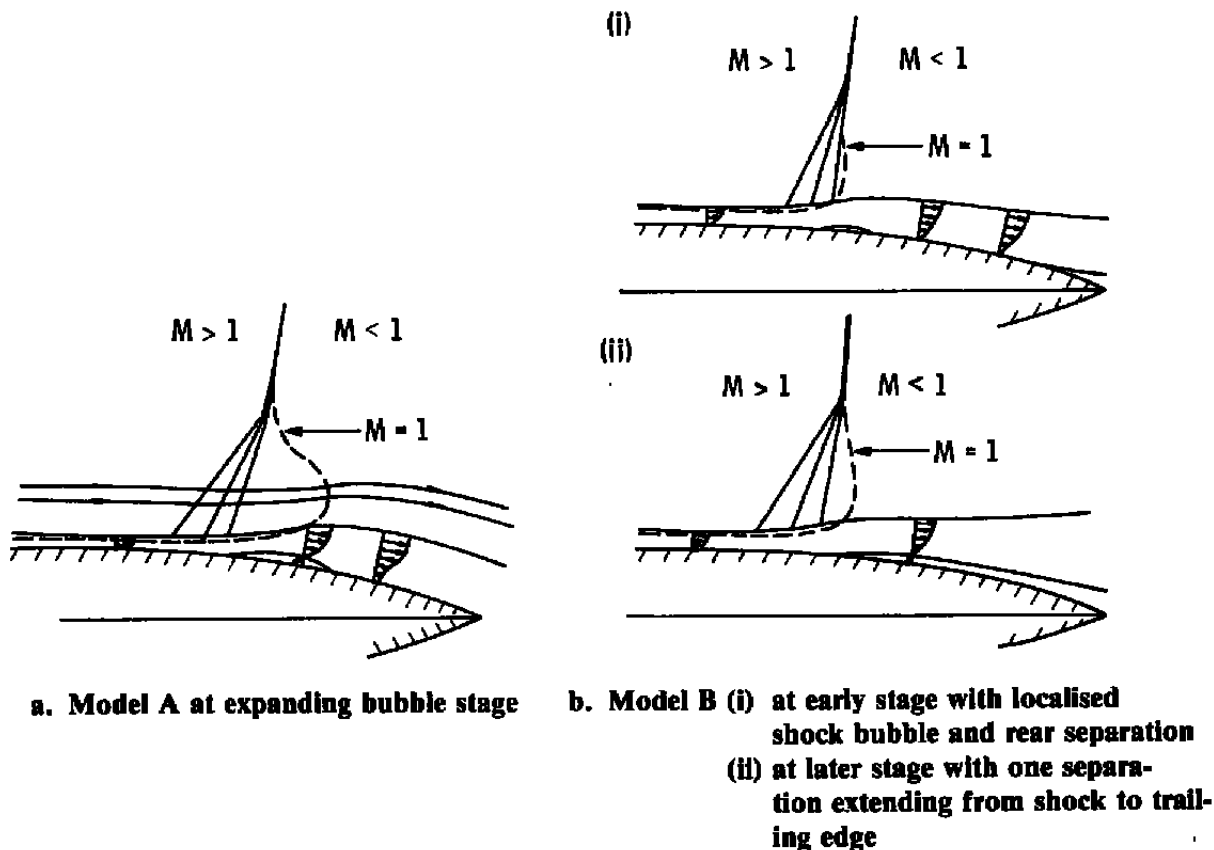


Figure 2. Some details (schematic) of the region of interaction between turbulent boundary layer and shock wave.
From Pearcey et al. (Ref. 2)

Green (Ref. 5) surveyed the work on SBL interactions published prior to 1969 and concluded that the influence of Reynolds number (Re) on pressure rise caused by a "free interaction" was unclear, particularly for very high Re . He stated that the then common assumption of $C_p Re_x^{1/10} = \text{constant}$ at given Mach number could lead to serious errors if applied over a wide range of Re_x . Green further suggested the interim adoption of the Reshotko and Tucker (Ref. 6) estimate of shock pressure rise based upon the relation (for turbulent flow),

$$M_2/M_1 = 0.762 \quad (1)$$

where M_1 , M_2 = local Mach numbers upstream and downstream of the shock, respectively. The pressure ratio following from Eq. (1) is determined by reference to oblique shock tables for the initial Mach number, M_1 . Although this procedure implies negligible effect of Reynolds number, it should be noted that turbulent boundary layer properties enter into the derivation of Eq. (1), and it is only by assuming constant values of the transformed shape parameter, \bar{H} , before and after the pressure jump that dependence on Re_x is avoided. Green suggested that \bar{H} should vary with Reynolds number but that the functional relationship was not clear at the time of his 1970 publication.

Original Model A
(Only Rearward Growth of Bubble)

VARIANTS OF ALTERNATIVE MODEL B
(Applicable When Rear Separation Is Incipient or Present)

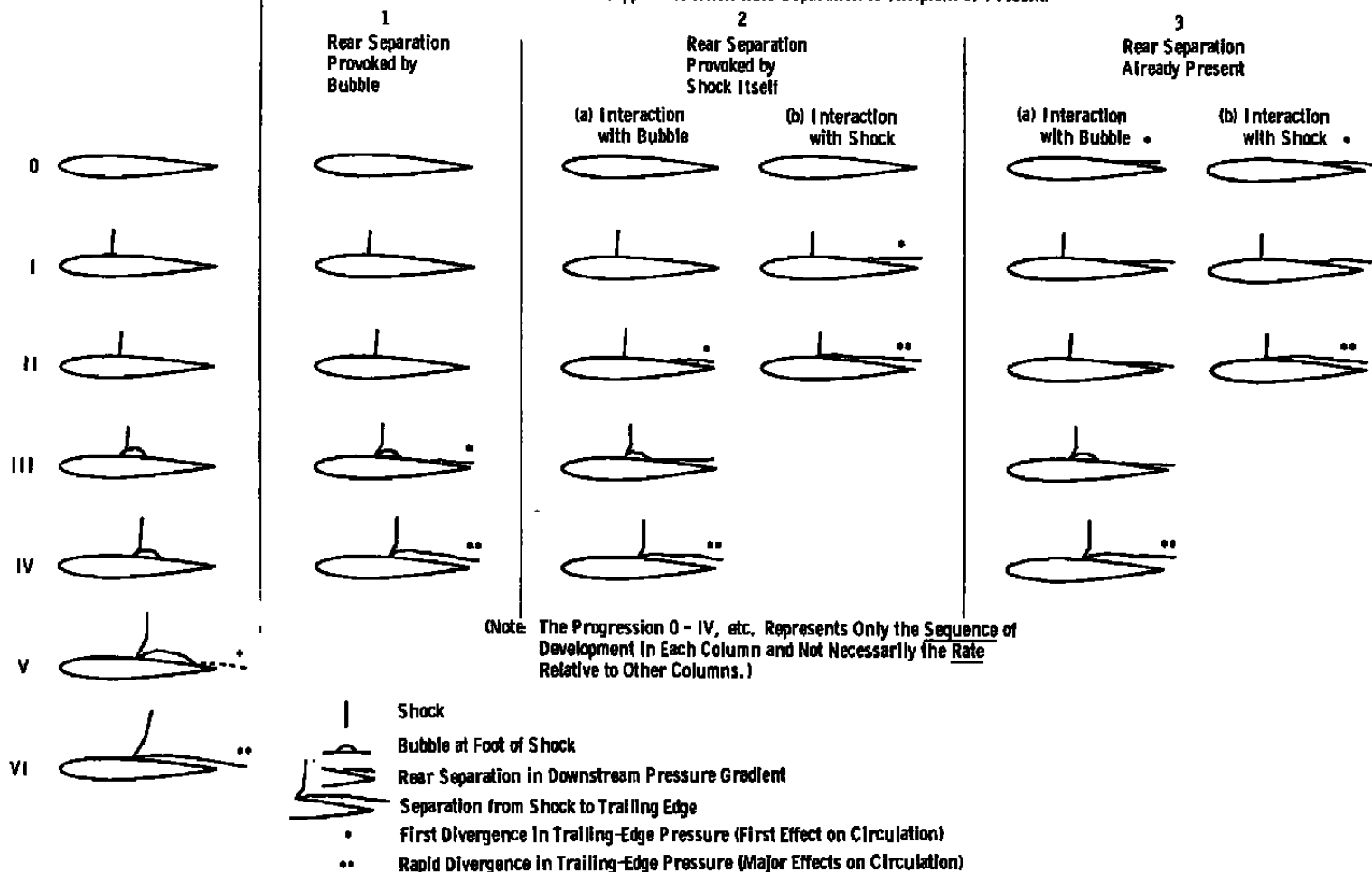
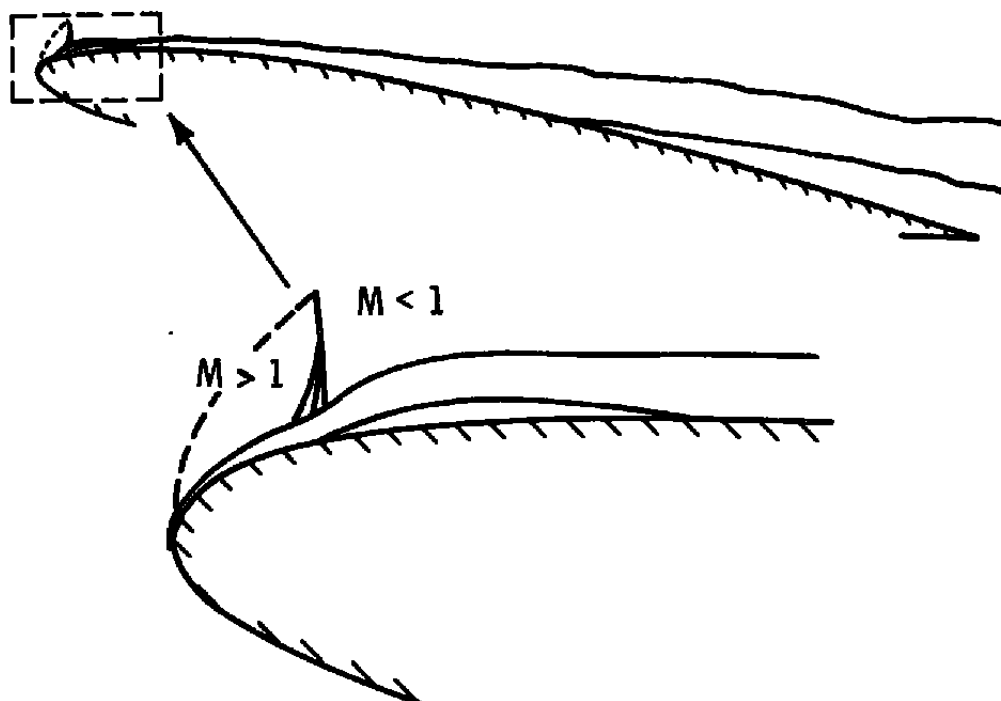


Figure 3. Flow models for the initial development of shock-induced separation (schematic); turbulent boundary layers (Successive stages in a Mach number or incidence increase). From Pearcey et al. (Ref. 2)



**Figure 4. Flow Model B in the particular form under consideration.
From Osborne and Pearcey (Ref. 3)**

When Green returned to this subject in his 1971 paper (Ref. 7), he presented the qualitative picture in Fig. 5, which is based on fragmentary data from several different investigators. Then, further to the question of shock-induced separations, Green made the point that values of Re_δ at a shock at, say, 40-percent chord on a model and a full-scale wing often can lie on either side of the transition between "low" and "high" Re_δ . Green made it clear that Fig. 5 was somewhat conjectural, and systematic data were lacking at the time of writing. Since that date, Settles et al. (Ref. 8) have presented data that indicate no Reynolds number effect on two-dimensional (2-D) ramp angles for incipient separation when $Re_\delta > 10^5$ (at $M_\infty = 2.9$). The more recent data do, however, show an influence of Re_δ on extent of upstream influence represented as $\Delta x/\delta_1$. For constant M_∞ intensity and ramp angle, raising Re_δ lowered $\Delta x/\delta_1$. Assuming $\Delta x/\delta_1$ to represent scale of separation, this appears to confirm the trend of curve (b) at larger Re_δ in Fig. 5.

The surge in computational fluid dynamics (CFD) during the past decade has produced a number of papers on viscous-inviscid interactions. Good examples include the review by Melnik (Ref. 9) and other work reported in the same conference proceedings. Melnik has presented CFD solutions for "weak" shocks that depend on Cole's wake parameter and a normalized shock strength parameter,

$$\chi_t \equiv (M_\infty^2 - 1)/\epsilon \quad (2)$$

where $\epsilon = u_*/U_e$ and $u_* =$ friction velocity $= 0$ (in Re) $^{-1}$, or a viscous, transonic similarity parameter,

$$K_t = \chi_t / [(\gamma + 1)M_\infty^2] = \frac{M_\infty^2 - 1}{(\gamma + 1)M_\infty^2 \epsilon} \quad (3)$$

where $\epsilon = (c_{f1}/2)^{1/2}$. The weak shock limit is defined as $\chi_t = 0(1)$, but results are given for higher χ_t values. These results display a Reynolds number or scale influence. Low χ_t , corresponding to larger c_{f1} at fixed M_∞ (lower Re) and all-turbulent flow, leads to greater calculated upstream influence.

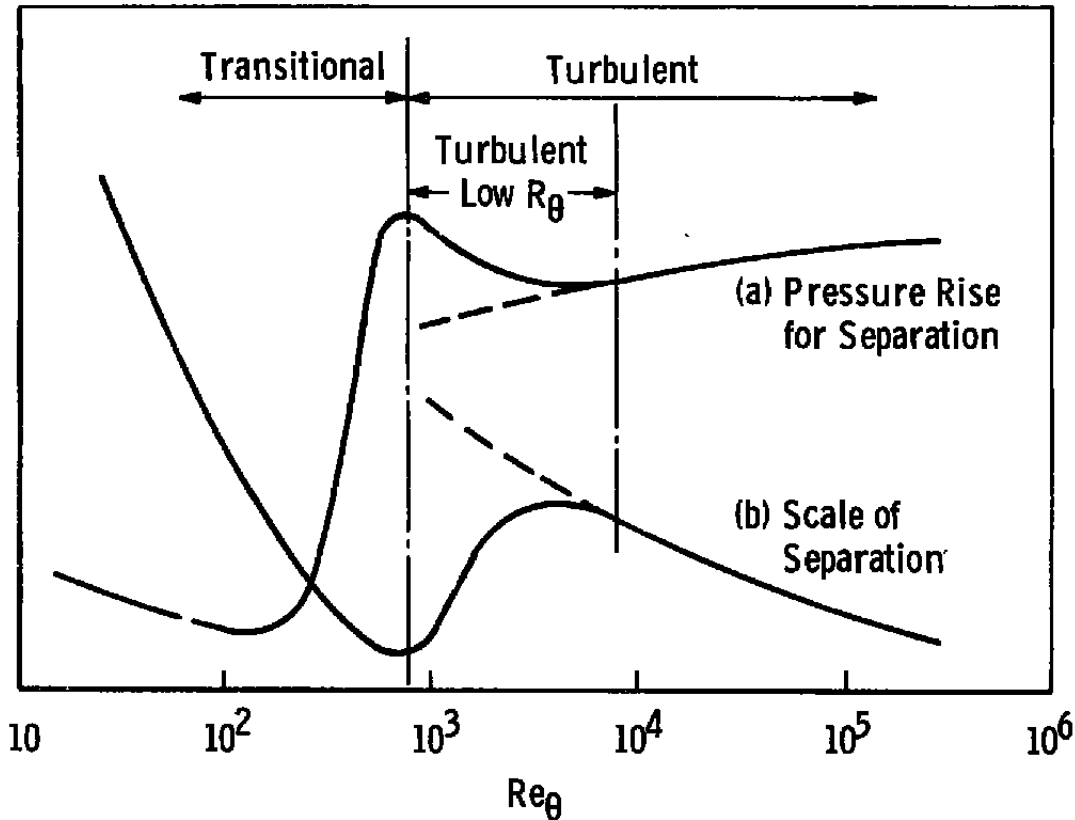


Figure 5. Influence of Reynolds number on the properties of shock-induced separation at Mach 1.5 (conjectural). From Green (Ref. 7)

2.2 THE CASE OF SWEEPED WINGS

The problem already seems severe enough without considering the added complications presented by swept, finite wings. In addition to Refs. 5 and 7, the SBL interaction in 3-D wing flows has been reviewed by Hall (Ref. 10) and Haines (Ref. 11), to name two notable examples.

The formidable challenge of 3-D transonic flows is apparent when the basic shock wave pattern of Fig. 6 is seen to lead to the complexity of Figs. 7 and 8 which are taken from Ref. 5, and Fig. 9, from Ref. 10. Leading-edge separation and vortex formation (Fig. 10) is equally daunting. These sketches and the spatial variation that may exist on a wing should be kept in mind when the application of boundary layer trips or other controls is discussed.

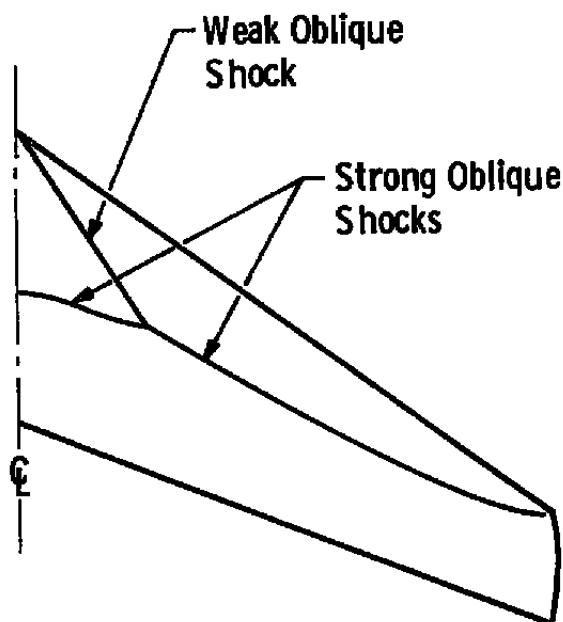


Figure 6. Basic shock pattern. From Hall (Ref. 10)

2.3 THE UNIT REYNOLDS NUMBER

It is important to note that a form of unit Reynolds number (U/ν) effect has been found in SBL-interaction experiments wherein that quantity and wetted length or boundary layer thickness were varied independently. A constant Reynolds number based on a wetted length still leaves boundary layer thickness as a variable influencing separation pressure rise and extent of separation. Stanewsky and Little (Ref. 12) presented data on 2-D airfoils showing effects of unit Reynolds number and mode of transition (natural and tripped) on pressure rise, separation bubble, and extent of rear separation. They reported that, for incompressible turbulent boundary layers,

If unit Reynolds number is held constant and δ is increased, C_{p_s} (separation pressure coefficient) will decrease with increasing Re_δ (Re based on boundary layer thickness upstream of shock). On the other hand, if one holds plate length, for instance, constant and increases unit Reynolds number, C_{p_s} will increase. (Halligan, internal Lockheed-Georgia Company report given as source.)

However, the variation of C_{p_s} with Re_δ shown in the analytical results is modest, being on the order of 10 percent for each factor of 10 in Re_δ . Reference 12 also includes data showing that extent of rear separation in compressible flow over an airfoil decreased with increasing unit Reynolds number and increased with increasing boundary layer thickness.

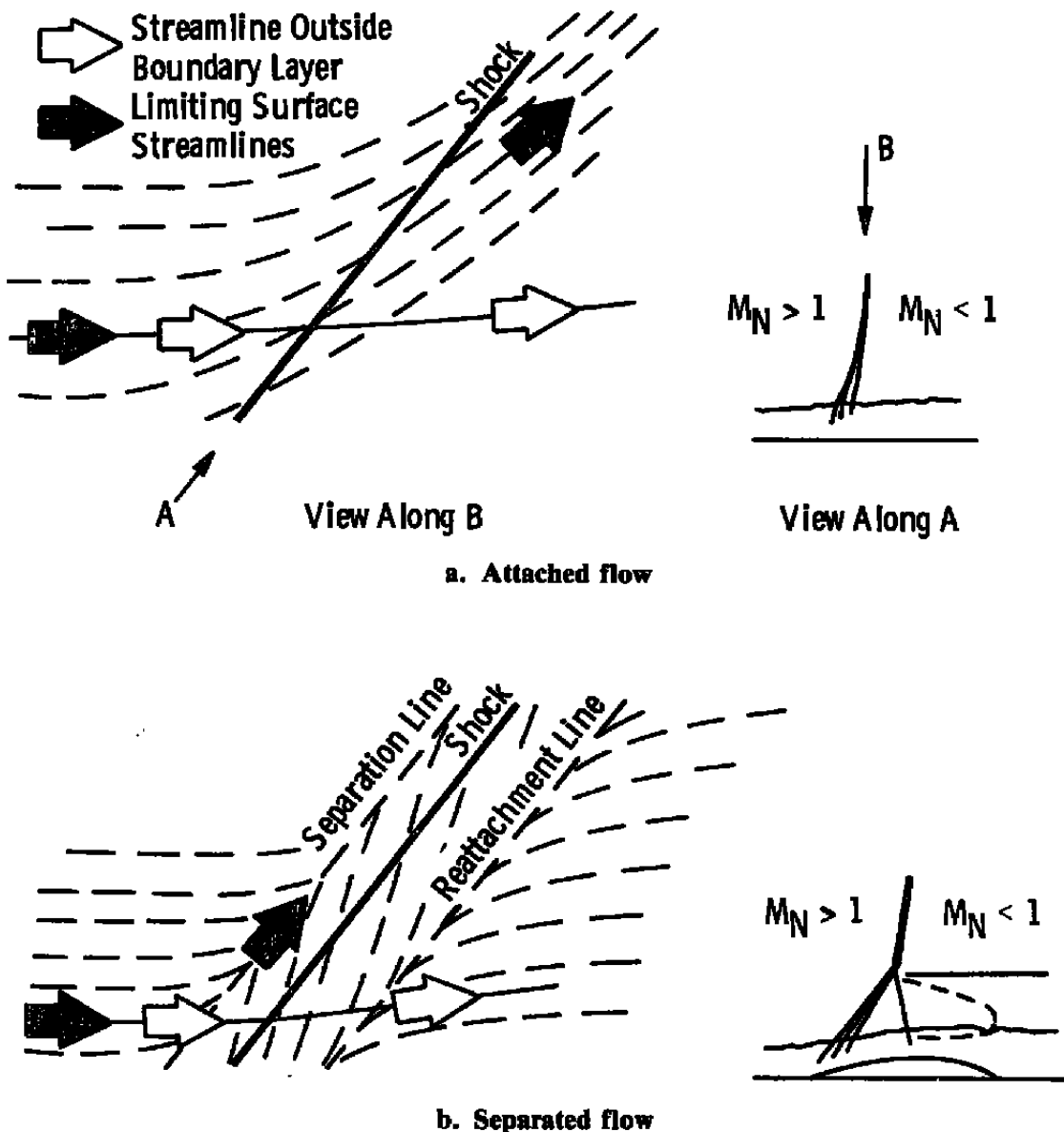


Figure 7. Surface flow beneath swept shocks. From Green (Ref. 5)

Settles et al. (Ref. 13) have found that 2-D, turbulent, compressible SBL interaction at a compression corner has an upstream influence distance, L_m , that scales according to the relation,

$$L_m(U/\nu)_1^{1/3} \delta_1^{-2/3} = (L_m/\delta_1)(U\delta_1/\nu)_1^{1/3} = \text{const} \quad (4)$$

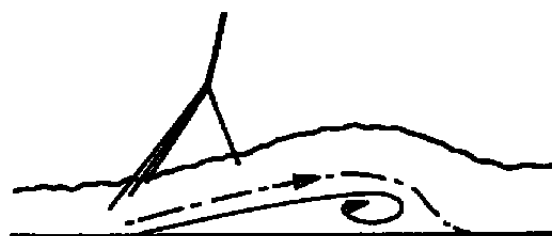
where δ_1 is the thickness of the undisturbed boundary layer at the corner for fixed M_1 and corner-ramp angle. Based on data and dimensional analysis, the same investigators propose another, more complex relation for 3-D flows,

$$L_m(U/\nu)_1^{1/3} \delta_1^{-2/3} = f \left[z(U/\nu)_1^{1/3} \delta_1^{-2/3}, \alpha, \lambda, M_1 \right] \quad (5)$$

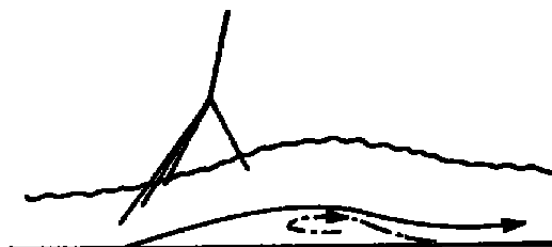
where δ_1 is the same as δ_1 except it now may have a spanwise variation. The spanwise coordinate is z ; λ is the sweep angle of the ramp; and α is the ramp angle.



a. Shock parallel to leading edge on infinite yawed surface



b. Conical flow



c. Tapering swept wing

Figure 8. Separation beneath swept shocks. From Green (Ref. 5)

In the simpler case of 2-D flow, the Ref. 13 results show that upstream influence, i.e., beginning of separation, scales as $\delta_1^{2/3}$ if $(U/\nu)_1$ is held constant, but L_m will decrease as $(U/\nu)_1^{1/3}$ increases while δ_1 or wetted length remains fixed.

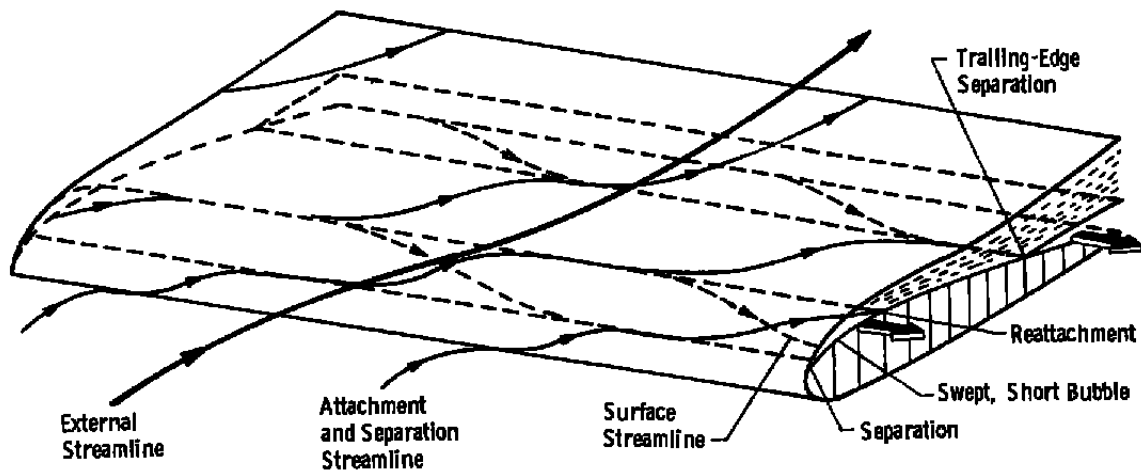


Figure 9. Flow pattern for swept, short bubble and trailing-edge separation. From Hall (Ref. 10)

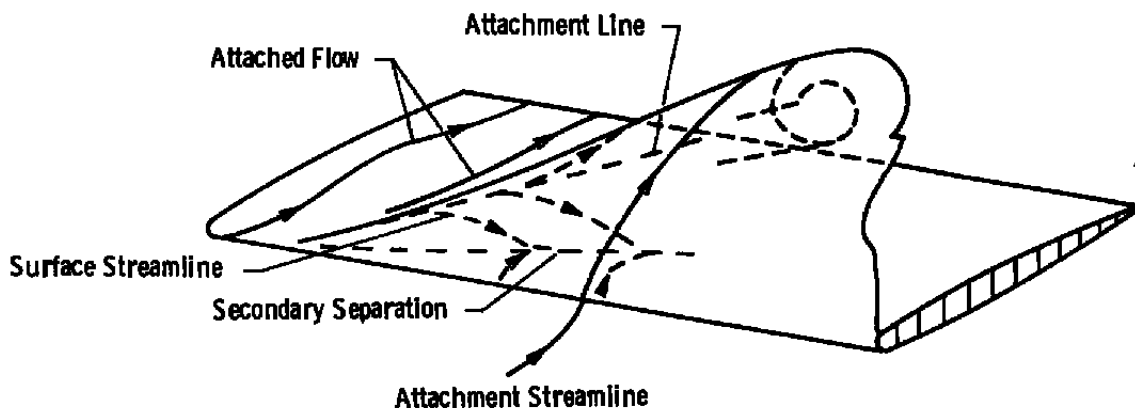


Figure 10. Flow pattern for vortex separation. From Hall (Ref. 10)

2.4 LOCATING THE TERMINAL SHOCK WAVE

Duplication of the full-scale shock position relative to the chord or other relevant length is a primary criterion for successful simulation. It is not the only criterion, but it clearly is one of the foremost requirements. If one is to do that, it is necessary to have some method for predicting where the shock will be under flight conditions. Therefore, it is fortunate that substantial progress in that area has been made. Cahill and Connor (Ref. 14) and, more

recently, Khan and Cahill (Ref. 15) have presented a method to predict the effects of changes in Reynolds number on pressure distributions, once the distributions are measured at lower Reynolds numbers.

In Refs. 14 and 15, trailing-edge pressure coefficient ($C_{p_{te}}$) is used as an indicator of significant trailing-edge separation. Such separation typically causes the shock to move forward. For a given Mach number, a single curve of $C_{p_{te}}$ versus shock location, in percent of chord, (x_{csh}) is shown to correlate a large amount of tunnel and flight data. These correlations are, of course, very sensitive to Mach number when that factor is near unity. The parameter used in Ref. 15 is given in Eq. (6). [See also Ref. 9 and Eq. (3) of this report.]

$$K = \frac{(M_e^2 - 1)}{(\gamma + 1)^{1/2} \epsilon M_e^2} \quad (6)$$

where $\epsilon = (c_f/2)^{1/2}$, and M_e is the local Mach number normal to a constant percent-of-chord line. Both M_e and c_f are the values immediately upstream of the terminal shock.

It is necessary that data be available for use in drawing the x_{csh} versus $C_{p_{te}}$ curve over some range of Re for a given airfoil or wing station and Mach number. The parameter, K , is calculated from the measured airfoil pressure distributions at various Re , supplemented by an appropriate skin-friction computation procedure. These results enable plotting a single curve of $C_{p_{te}}$ versus K , which will resemble the example shown in Fig. 11. The break-point coordinates (K_0 , $C_{p_{teo}}$) reflect the Reynolds number influence. Thus, Ref. 15 contains curves of ΔK_0 and $\Delta C_{p_{teo}}$ versus Re_c , where the latter is based on local wing chord and the Δ 's indicate change from the values when $Re_c = 10^7$. The experimentally and computationally determined curve of $C_{p_{te}}$ versus K is shifted to correspond to higher Re_c by replotting in $(C_{p_{te}} - C_{p_{teo}})$, $(K - K_0)$ coordinates and using the ΔK_0 and $\Delta C_{p_{teo}}$ correlations of Ref. 15 to predict the Reynolds number effect. The C_p at the beginning of the shock is calculated using K , M_∞ , and c_f , with the stipulation that the local Mach number normal to the element lines of the wing planform at the foot of the shock is unity.

The procedure is inapplicable in cases where a local separation bubble occurs at the shock, or low-speed stall occurs. The latter situation is identifiable with a smoothed-out compression originating near the leading edge and no evidence of a discrete shock. The correlation is restricted to moderate angles of attack. In those cases where separation bubbles lie at the foot of the shock, significant scale effects are not anticipated if a turbulent boundary layer exists at the shock. Although the referenced work does not cover every condition encountered in simulating full-scale flows, it does provide an approach for a large class of flows. Time will tell if other users find the method to hold up when still more applications are tried.

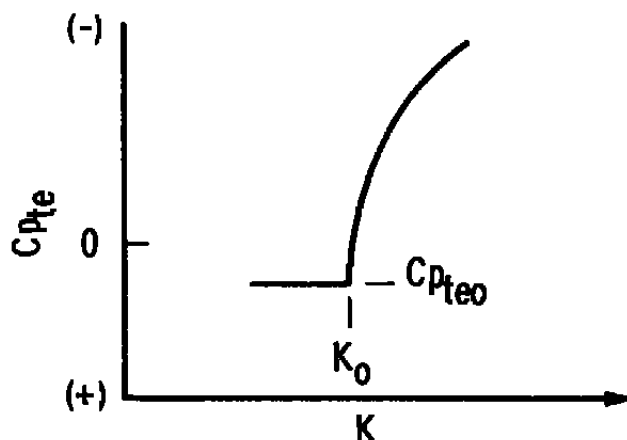


Figure 11. Trailing-edge pressure coefficient as a function of correlation parameter K. From Khan and Cahill (Ref. 15)

2.5 VORTEX SEPARATION

It has been shown that a swept wing may experience separation in the form of swept, short bubbles, trailing-edge separation, and vortex separation. Combinations or multiple examples of these phenomena may be present at one time. All of the discussion thus far has concerned the first two forms because less has been written about scale effect on vortex separation. As Hall has remarked (Ref. 10), there will be some influence of Reynolds number whenever there is flow separation, and the amplifying three-dimensionality as separation spreads on swept wings poses an especially tricky simulation problem.

Leading-edge separation and vortex formation may be expected for thin, swept wings at rather low angles of attack. Depending on the local Mach number, there may also be shock waves in that region. Thus, complicated flows and potentially significant effects involving vortices, vortex-shock interactions, and other forms of flow separation may be encountered. An appreciation of this type of flow may be gained by examining Figs. 6, 7, and 8 in the paper by Moss (Ref. 16).

When tests are conducted in wind tunnels at relatively low Reynolds numbers, the boundary layer may be laminar where the vortex forms near the leading edge. If the full-scale boundary layer is turbulent in the same region, differences between the wind tunnel and full-scale pressure distributions can be expected. The overall effect of this will vary with the particular circumstances, and it cannot be assumed that the application of boundary layer trips offers a satisfactory solution. The thinness of the boundary layer near the leading edge makes it likely that the use of conventional 2- or 3-D roughness for tripping will cause too much thickening of the boundary layer and interact too strongly with the vortex and

shock when those are present. A trip suitable for attachment to leading edges without significant thickening of the boundary layer obviously would be valuable. Some suggest that trips should be at least 15 percent of chord upstream of a shock wave.

Rogers and Hall (Ref. 17) and Squire (Ref. 18), for example, show that separation and vortex formation on wings with highly swept leading edges occur at very low angles of attack, particularly near the tip. Figure 12 from Ref. 18 illustrates this in the case of a delta wing with aspect ratio of 4/3 and Reynolds number based on root chord of 10^7 . Kuchemann (Ref. 19) has discussed vortex and separation formation generally. He has stated that Reynolds number cannot affect the general character of the various vortex patterns on swept-back wings but that it will greatly influence the changeover from one type of flow to another, as well as shape and stability of the vortex sheets. In a valuable review of separation, Smith (Ref. 20) has written that,

If the separation takes place from a salient edge, its occurrence is independent of the boundary layer structure, at least for high Reynolds number. A shear layer forms at the salient edge, and again for high Reynolds number, this can be modeled by a vortex sheet. The role of viscosity is to produce the separation; its location is determined geometrically. Inviscid models can then be constructed.

Hummel (Ref. 21) has presented data for delta wings with sharp leading edges in subsonic flow showing that the pressure distributions were different for laminar and turbulent boundary layers. However, the integrated pressure distributions were about equal, and he concluded that the overall characteristics of slender delta wings are independent of Reynolds number.

Polhamus and Gloss (Ref. 22) stated that,

The origin of the primary vortex feeding sheet and its feeding rate are sensitive to Reynolds number, especially for the rounded leading-edge case and for the secondary vortex regardless of the leading-edge condition. Both the symmetric and asymmetric vortex breakdown characteristics, which play an important role in high angle-of-attack stability, are Reynolds number dependent.

They also remarked that the vortex feeding sheet remains fixed at sharp leading edges, and therefore, the major features of the flow are not critically dependent on Reynolds number in that case. They presented the data in Fig. 13 to illustrate Reynolds number effect on a wing. Figure 14 is reproduced from Ref. 23 to clarify the primary and secondary vortices referred to by Polhamus and Gloss.

In Fig. 13 it will be noted that, although the Reynolds number effect is concentrated over the forward 16 percent of the wing, the change in pressure distribution is marked when the vortex is affected.

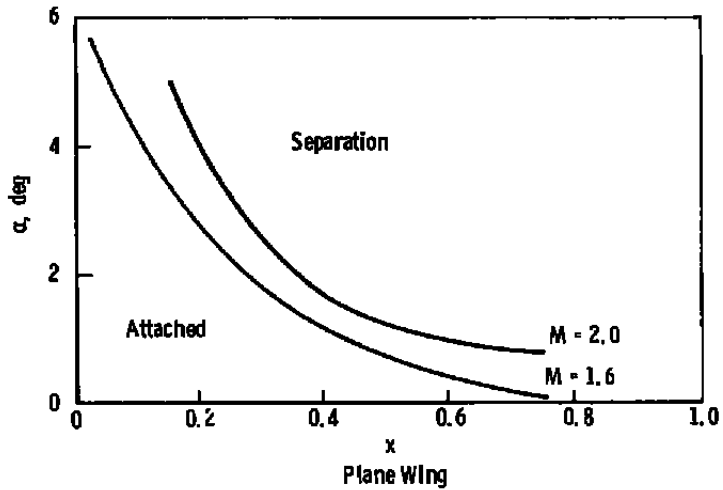
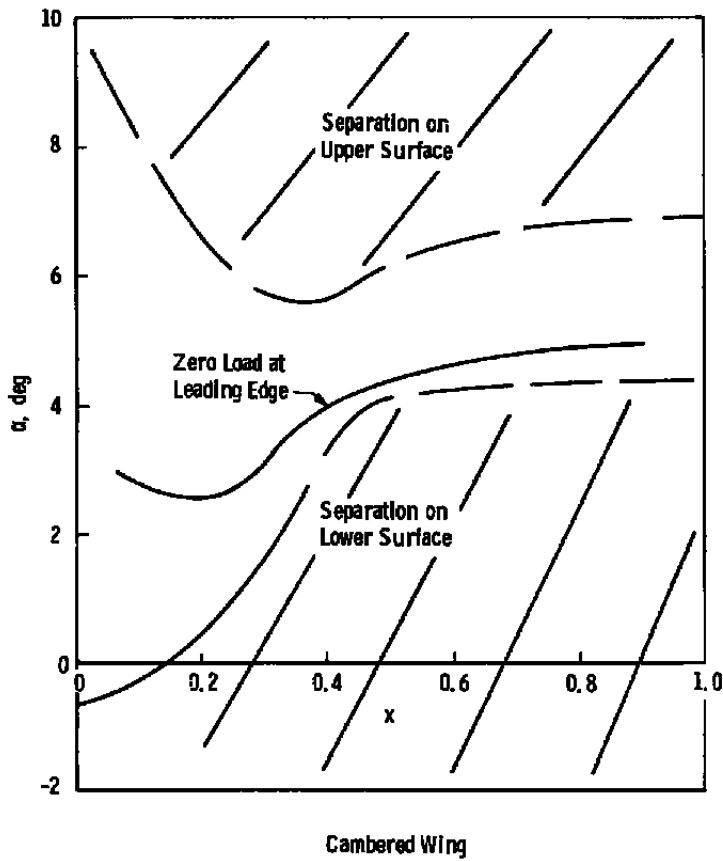


Figure 12. Leading-edge separation boundaries on plane and cambered wing of aspect ratio 4/3. From Squire (Ref. 18)

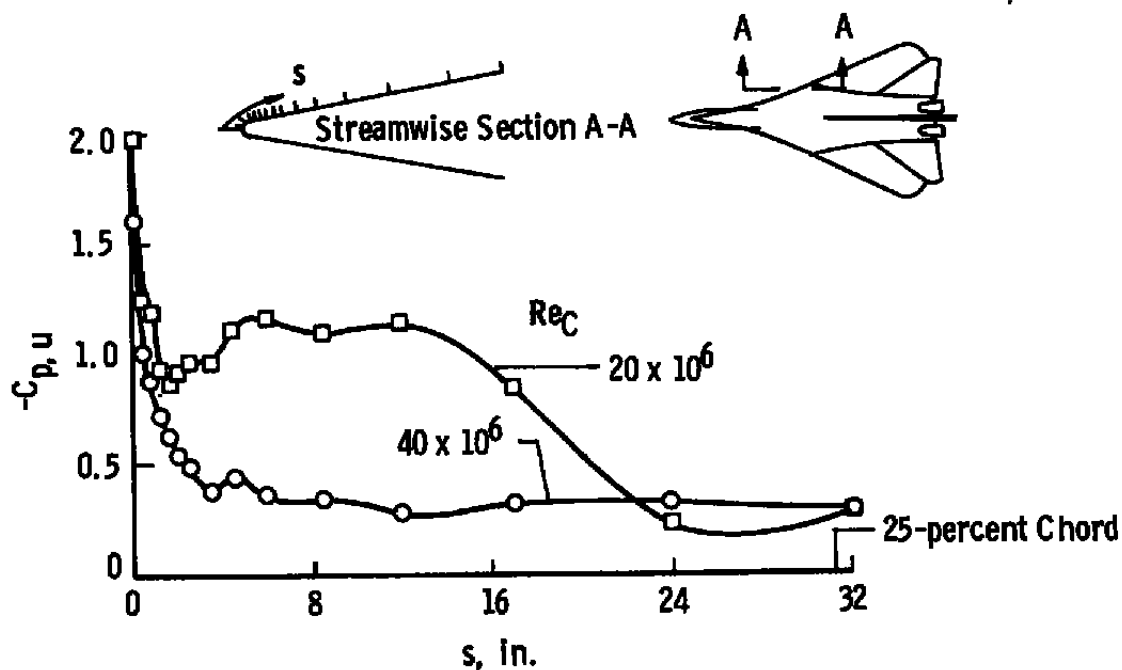


Figure 13. Effect of Reynolds number on vortex-flow development — F-111 TACT flight experiment; $\alpha = 6$ deg, $M_\infty = 0.6$. From Polhamus and Gloss (Ref. 22)

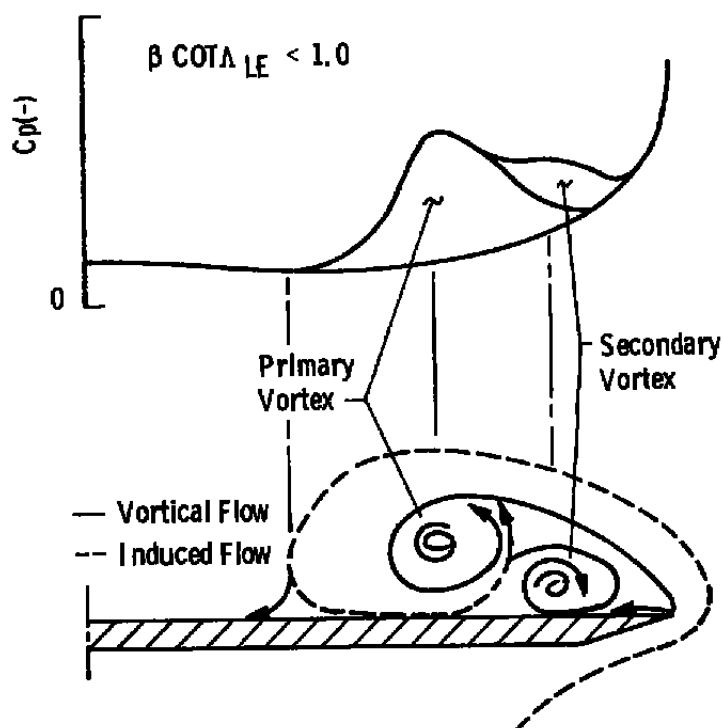


Figure 14. Classical leading-edge vortex characteristics. From Miller and Wood (Ref. 23)

Miller and Wood (Ref. 23) present data on surface flow patterns and pressure distributions near the trailing edges of delta planforms in supersonic flows for various vortex conditions. The interaction between vortices and shock waves in supersonic flow is illustrated, and the areas wherein the different forms of vortex-shock interaction which may be encountered are mapped in terms of angle of attack and Mach number normal to the leading edge. Reynolds number variations apparently were not investigated.

Figure 15, after Waggoner (Ref. 24), illustrates again that an influence of Reynolds number can be significant when vortical flows are involved. It also shows that very large ranges of Reynolds number may be required for investigation of this type of flow.

The seeming contradictions in these reports can only be partially explained. Hummel's data pertain to a sharp, flat wing at $\alpha = 20.5$ deg, and $Re_c = 0.9 \times 10^6$ in low-speed flow. The "salient edge" concept clearly should be applicable in that case, and vortex breakdown had not occurred. The data in Fig. 13 pertain to an aircraft at $M_\infty = 0.6$, with a finite leading-edge radius, $\alpha = 6$ deg, and $Re_c = 20 - 40 \times 10^6$. The concept of a salient edge is at least questionable in this case, and one would have to suspect that the higher Reynolds number brought about vortex breakdown and the loss in suction shown in Fig. 13.

A finite leading-edge radius also characterizes the model in Fig. 15. Even though the angle of attack is 10 deg, it appears that the flow is approaching an attached condition as Re increases. The low Mach number assures that shock-induced separation is not a factor.

In the context of this report, it is inferred that a scale effect should be expected if the higher Reynolds number that one wishes to simulate is sufficient to change the basic character of the flow. That can occur if shock interaction is significantly changed or if vortex breakdown is precipitated as Reynolds number increases. It will sometimes be feasible to approximate the subsonic, high- Re limit by computing the inviscid, attached-flow values of the aerodynamic coefficients.

It is well known that fuselages or missiles at high angles of attack may experience yawing moments and side forces created by asymmetrical vortices shed from the inclined body. Evidence of Reynolds number effects has been presented, cf. Keener et al. (Ref. 25) or Jorgensen (Ref. 26). The data show that quite unexpected effects are likely to arise from attempts to simulate higher Reynolds numbers by using boundary layer trips. Figure 16, taken from Ref. 26, shows that increasing Reynolds number affected side forces in a dramatic fashion. However, either longitudinal strips of roughness or grit applied to the nose of a body of revolution have been found to diminish side forces or yawing moments

when they are located so as to cause symmetrical separation and vortex production. It is obvious that simulation of higher Reynolds numbers by the use of trips almost surely would not have yielded the same results as are shown in Fig. 16, and it is clearly dangerous to use trips in any case where vortex strength and location may be directly influenced by proximity of the trips. Forces and moments arising from asymmetric vortex patterns often will have unpredictable, random signs depending on minute model construction flaws, support misalignment, or free-stream flow asymmetries. Testing methods and data interpretation are especially critical when this type of flow exists.

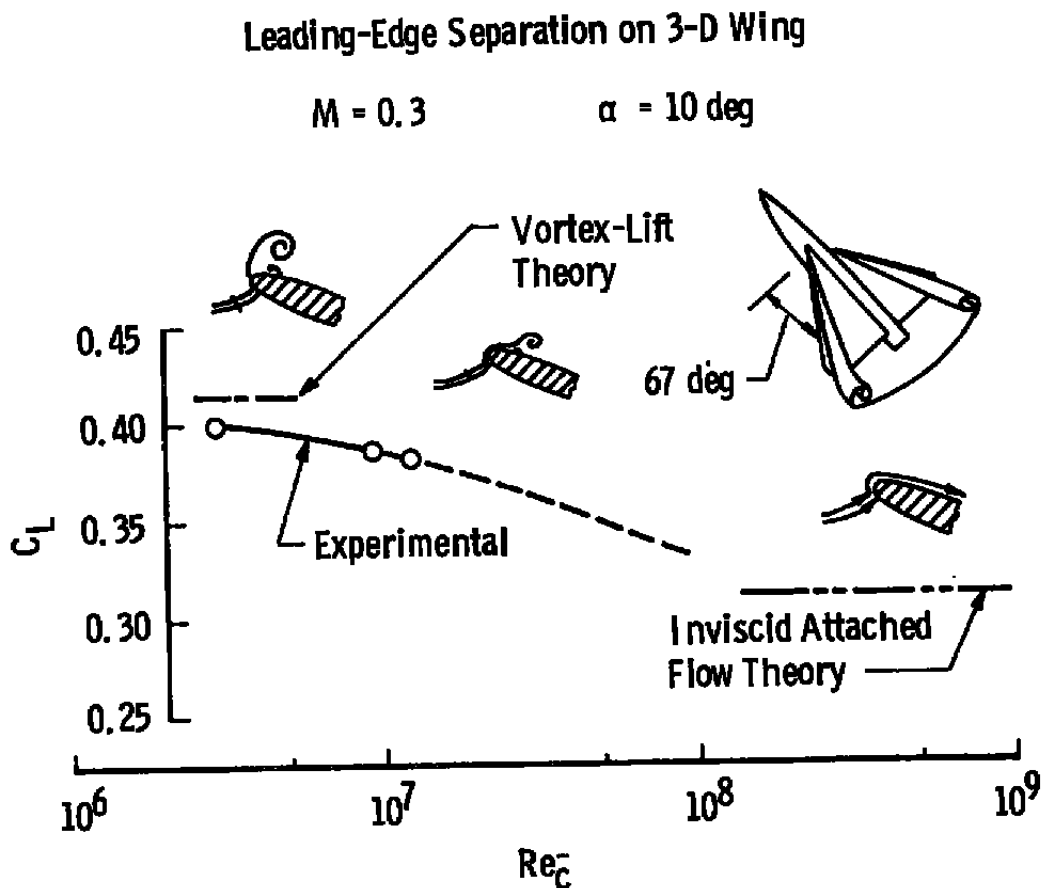
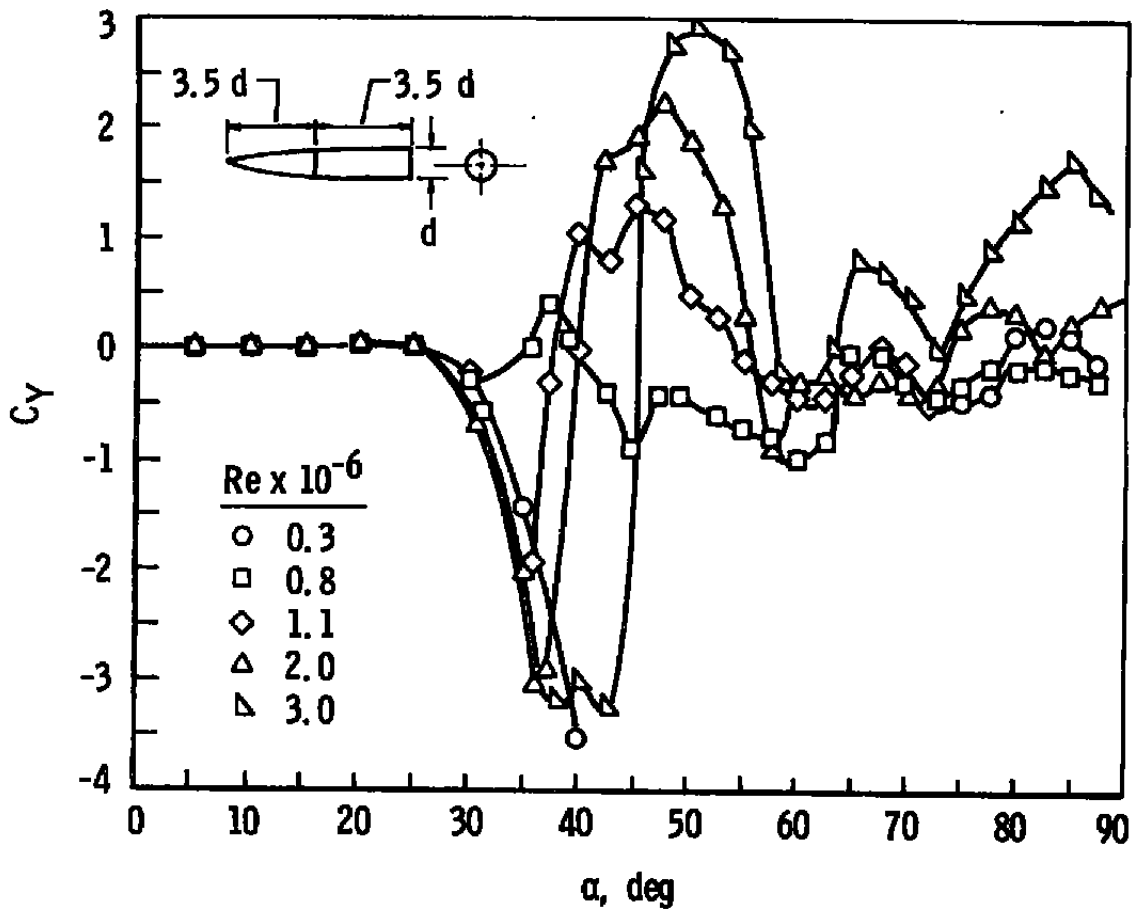
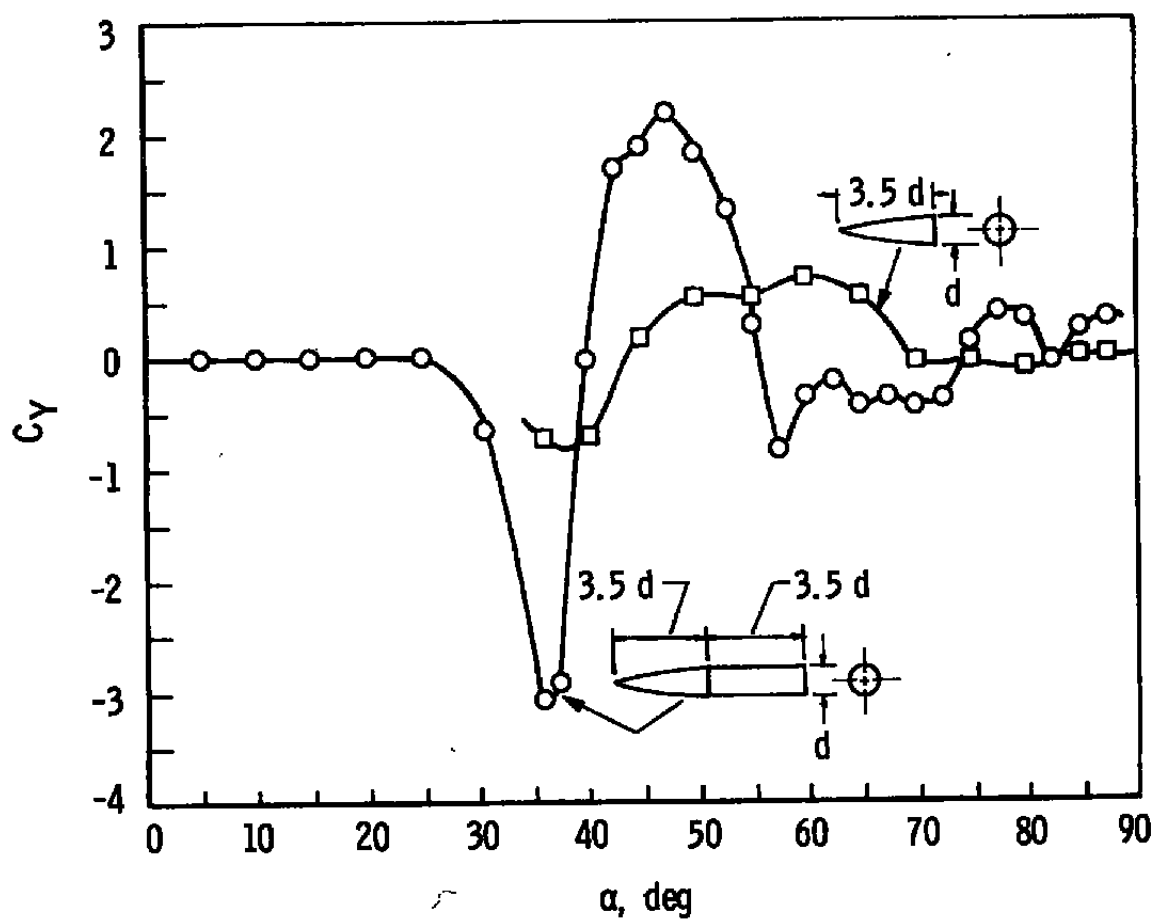


Figure 15. Variation of lift coefficient with Reynolds number where leading-edge separation and vortical flow exist. From Waggoner (Ref. 24)



a. $M_\infty = 0.25$

Figure 16. Effect of Reynolds number on side-force coefficient for an ogive-cylinder body of revolution. From Jorgensen (Ref. 26), credited to Keener (Ref. 25)



b. $M_\infty = 0.25$, $Re = 2.0 \times 10^6$
 Figure 16. Concluded.

3.0 SIMULATION REQUIREMENTS

Earlier investigations of techniques for coping with transonic SBL-simulation deficiencies have led to various recommendations and warnings. In general, there is agreement that,

An essential requirement of model-scale testing is to reproduce the full-scale location of the shock wave. (Pankhurst, Ref. 27)

To that end, it has been recommended that first priority be given to making the boundary layer turbulent at the foot of the shock (if that full-scale condition is expected). Recalling that Pearcey et al. (Ref. 2) defined Model A and B flows which have differing simulation requirements, we note that the principal requirement for Model A flows is that the turbulent boundary layer condition be provided. Transition must be complete upstream of the shock, but it need not be as far forward as it is in full-scale. This will allow closer approximation to $(\delta/c)_{\text{full-scale}}$ by making $(x_t/c)_{\text{model}} > (x_t/c)_{\text{full-scale}}$ even though $Re_{c \text{ model}} < Re_{c \text{ full-scale}}$.

The dismissal of Reynolds number-related effects in the cases of unseparated flows and Model A flows with bubble separations may be permissible in regard to shock position, but there are Reynolds number effects on skin friction and wake which should not be ignored (cf. Refs. 7, 10, and 28). This is summarized as follows:

As long as there is no separation, the behaviour of the boundary layer in the region of interaction does not appear to have an appreciable, direct effect on the position of the shock wave. Also, the difference between the actual pressure distribution and one with a discontinuous pressure rise at the shock position has little effect on the lift, drag, and pitching moment of the aerofoil. However, boundary-layer behaviour through the interaction does have an effect on the subsequent development of the boundary layer and wake and hence, via the weak, overall interaction, it does have some influence on the flow field at large. (Green, Ref. 7)

If separation is not present, the shapes of the velocity profiles in the boundary layers approaching the trailing edge on the upper and lower surfaces are the key features to simulate, according to Green. In an investigation reported by Blackwell (Ref. 29) where a "small amount" of shock-induced separation was said to exist, substantial Reynolds number effects were found, and the recommendation was to simulate the boundary layer characteristics at the airfoil trailing edge. Matching the shape factor, H , was specifically recommended.

If Model B flows are involved, a good summary of the situation is the following:

The prime requirement for correct simulation thus remains a boundary layer that is turbulent at the point of interaction with the shock. It is now also clear, however, that there is a further requirement of almost equal importance and generality: this turbulent layer must be of a thickness that is *not* so magnified in relation to full scale (and must have a profile that is not so distorted) that after interaction with the shock it will provoke a rear separation that would not be present at full scale, or will increase significantly the severity of such rear separation as might be present at full scale. (Pearcey et al., Ref. 2)

The latter quotation is only a portion of the "Concluding Remarks" in Ref. 2, which should be read in its entirety for a valuable lesson on simulation problems of Model A and B flows.

Leaving aside the question of how one is to predict where the critical airfoil station may be in a given case, it still may not be possible to bring about the desired turbulent boundary layer thickness by using trips. Tripping can be supplemented by suction or cooling to thin the tripped layer, but the expense is obvious and there would remain a problem of accommodating varying test conditions without an elaborate boundary layer control system such as Green and Bore have discussed (Refs. 7 and 30, respectively).

The situation faced by experimenters who cannot meet all of the applicable simulation requirements necessitates that extra steps in testing and computation be taken if full-scale results are to be predicted. The procedure obviously is fraught with uncertainty, and there may be angles of attack or other conditions where no approach is going to be successful. Figure 17 shows the Reynolds number gap that may have to be bridged by extrapolation.

Basically, if subscale measurements can be made at conditions where reasonably well-behaved variations with increasing Reynolds number can be relied on, then theoretical and computational means can be used to perform the required extrapolation to higher Reynolds numbers. To carry this out, full-scale position of the shock wave(s) will have to be estimated, and boundary layer tripping usually will have to be used to approximate the desired boundary layer conditions at the shock. Transport aircraft wings will be affected mainly by Model A and B SBL-interaction effects, while the lower aspect ratios, higher angle-of-attack operations, thinner airfoils, and greater sweep of fighters and missiles often will make vortex-shock interactions important in simulation of those vehicles. Missiles and airplane forebodies at angles of attack also experience flow separation and vortex formation, with possible scaling problems in their testing (cf. Fig. 16).

In summary, the currently recognized requirements for simulating transonic, viscous flows are as follows (assuming equality of Mach numbers and accurately scaled models):

1. Create full-scale shock position, i.e., $(x/c)_{\text{model sh}} \approx (x/c)_{\text{full-scale sh}}$
 2. Have turbulent boundary layer at foot of shock if that is the full-scale condition
 3. Have $(\delta^*/c)_{\text{model}} \approx (\delta^*/c)_{\text{full-scale}}$
 4. Have $H_{\text{model}} \approx H_{\text{full-scale}}$
- } at shock
5. Create full-scale vortex relative position and strength if that is a feature of the flow

where δ^* = boundary layer displacement thickness; c = wing chord or other appropriate length; and H = boundary layer shape factor.

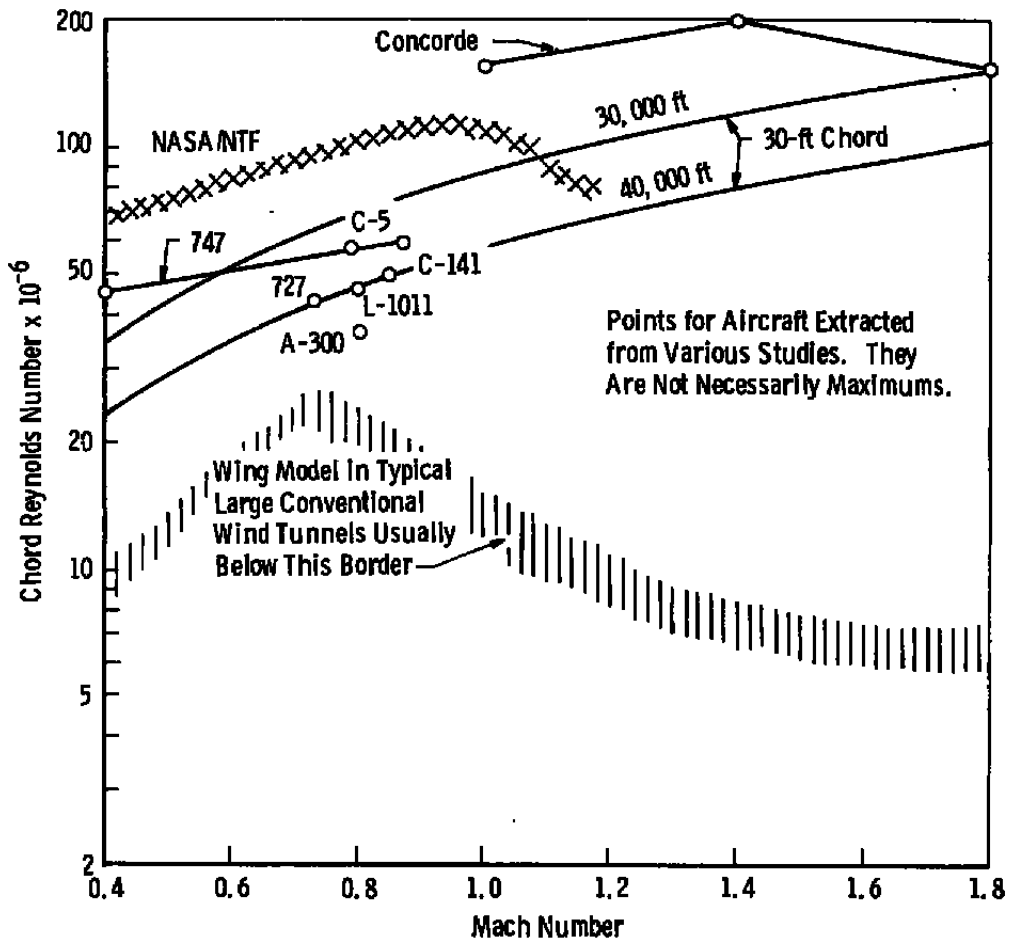


Figure 17. Wind tunnels and flight Reynolds number.

In this case, the "approximately equal" signs must be regarded as meaning "sufficiently close to." In typical aerodynamic testing, these requirements are seldom all met, and the foregoing list does not recognize the evidence that the unit Reynolds number affects SBL interaction. Of course, equality of model and full-scale unit Reynolds numbers in scale-model testing is incompatible with (1) and (3). Testing over a range of U/ν and varying model sizes would seem the only recourse. Number (3) becomes virtually impossible when $Re_{c \text{ model}} \ll Re_{c \text{ full-scale}}$ and boundary layer tripping is done, unless some auxiliary means of thinning the boundary layer is implemented. Number (4) seems within reach in many cases. Number (5) refers to a complex flow interaction which may be influenced by very small model or free-stream asymmetries such that the flow sometimes seems to have a random character. Requirements numbered (2), (3), and (4) have generally been considered the keys for satisfying requirement (1) and the type and extent of separation related to the SBL interaction on wings at low angles of attack. It is desirable to simulate full-scale boundary layer characteristics at the trailing edge, as well as at the shock, but one may not be able to do both. Meeting the listed conditions at the highest available $(U/\nu)_\infty$ may result in the closest approach.

It is important to be aware that significantly different flow conditions can exist within the general class of transonic flows. Small changes in Mach number can strongly influence viscous interaction; boundary layer transition is differently affected by sweep angle at different Mach numbers; roughness rapidly declines in effectiveness as Mach number increases in the region of $M_k \approx 1$; etc. Therefore, the experimenter seeking to establish dynamic similarity has to be careful of generalizations and be mindful of the particular case at hand.

Nothing has been said about the situation that will arise when vortices and/or wakes from canard surfaces interfere with wings. Whether unusual Reynolds number effects arise in such cases is not clear; no data have been noted. However, it is not difficult to visualize qualitative Reynolds number effects. Considering that configurations with gaps are sometimes encountered, it should be mentioned that equal (gap width/ δ^*) seems more important than geometrically scaled gap width in subscale testing.

4.0 INFLUENCING BOUNDARY LAYERS TO SIMULATE HIGHER REYNOLDS NUMBERS

4.1 BOUNDARY LAYER TRANSITION AND THICKNESS

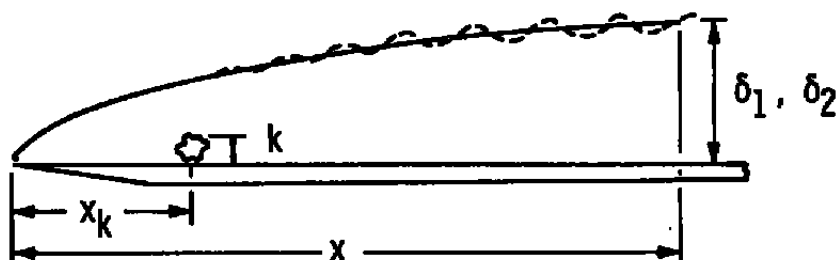
There have been recent and comprehensive reviews of boundary layer transition and the nature of disturbances created by single roughness elements. For that information, readers may turn to Refs. 31, 32, and 33. The specific concern with transition that is examined here is its manipulation so as to compensate for the deficiency in Reynolds number. The major

object is to bring about the shock location and boundary layer separation that duplicate what would occur in full-scale free flight. Often that requires moving transition forward to a station where it would occur naturally if the Reynolds number were greater. That relocation may be done by using boundary layer trips, but trips can cause excessive thickening of the boundary layer and prevent reproducing full-scale separation patterns. Trips may also cause extraneous drag when they are too large. Thus, tripping the boundary layer at the desired location is not the only requirement; it must be done with minimal loss of energy and extraneous drag.

Peterson (Ref. 34) measured boundary layer profiles relatively far downstream of trips ($x/k = 430$ to 4560), with results such as are shown in Table 1. Narrow-band grit roughness is represented in these data, which suggest that thickening of the boundary layer is insignificant when $k/\delta_k \lesssim 1/2$ and $x \gg k$. It is also encouraging to note that the shape factor is unaffected, even when $k > \delta_k$. Subscript 1 means no trip; 2 means with trip.

Table 1. Data on Supersonic Boundary Layer Downstream of 3-D Trips. From Peterson (Ref. 34)

$M_e \approx 3.1, \delta_k = 0.015 \text{ cm}, x_k = 0.64 \text{ cm}, x = 21.6 \text{ cm}$				
k/δ_k	δ_2/δ_1	δ_2^*/δ_1^*	θ_2/θ_1	H_2/H_1
0	1.000	1.000	1.000	1.000
---	---	---	---	---
0.307	1.013	0.980	1.000	0.983
0.527	1.026	0.970	0.980	0.983
0.607	1.126	1.157	1.155	1.000
1.033	1.168	1.147	1.150	1.000
1.293	1.201	1.265	1.263	1.000
1.907	1.226	1.265	1.269	1.000
1.987	1.278	1.304	1.314	0.983
3.273	1.291	1.147	1.184	0.966



However, it must be emphasized that these data represent 3-D trips, Mach 3 flow, $x \gg x_k$ and $x \gg k$. Viewing the low-speed data of Klebanoff and Tidstrom (Ref. 35) reveals

that the boundary layer at stations only a short distance downstream of the roughness is affected by even very small trips. Figure 18 from Ref. 35 makes this point. The boundary layer thicknesses of the undisturbed laminar layer at the roughness station, x_k , are not given in Ref. 35, but calculated values for a Blasius layer are $\delta_k = 0.843$ cm, $\delta_k^* = 0.279$ cm (0.11 in.), and $\theta_k = 0.108$ cm (0.04 in.) for the condition corresponding to the square symbols. The shape factor, H , would be 2.59. Thus, Fig. 18 shows that δ^* immediately downstream of x_k is first greater than the untripped value; then it drops below that level, and it appears that it begins to increase when $x > 0$ (100 k). Momentum thickness, θ , just downstream of x_k is lower than its undisturbed level, and it slowly increases toward that level with increasing x . The shape factor, H , initially higher than the undisturbed laminar value, has attained the undisturbed value when $(x - x_k) > 0$ (100 k). Most transonic testing requires that $x_t \rightarrow x_k$.

The more general studies of tripping have concerned 2-D flows with no pressure gradients; thus, the results may not be directly applicable to cases encountered in testing many aircraft models. Reexamining Fig. 7 arouses suspicion that tripping criteria for swept 3-D wings differ from 2-D cases. A few of the possible factors in tripping 3-D boundary layers are briefly examined.

Regarding swept wings, there is some reason to hope that 2-D methods for sizing trips can be adopted successfully because of the independence principle. Based on the analysis of laminar, incompressible flows over yawed 2-D bodies, Prandtl (Ref. 36), Struminsky (Ref. 37), Jones (Ref. 38), and Sears (Ref. 39) have concluded that the streamwise flow is independent of the spanwise flow in such cases. There is experimental evidence that independence also prevails for the turbulent boundary layer (Ref. 40), but others have reached the opposite conclusion (Ref. 41). However, it is laminar flow that has to be tripped, and the independence principle offers justification for using the same method of trip sizing on both swept and unswept wings. It also offers encouragement that methods such as Refs. 42, 43, 44, 45, and 46 can be used if confined to the case where transition is wanted "near" the trip, i.e., $x_t \rightarrow x_k$. The latter statements are made even though the independence principle is not valid in boundary layer stability theory (Personal communication from Prof. Eli Reshotko of Case-Western Reserve University, November 1983). It is possible that stability considerations do not apply when a strong overriding disturbance such as trips brings about transition.

Evans (Ref. 47) examined the effectiveness of trips on several swept wings and found his data did not fit the predictions for 2-D, zero-pressure-gradient flows of Refs. 42, 43, 44, and 45. Specifically, the roughness was less effective than predicted by the methods of Refs. 43, 44, and 45, but more effective than predicted following Ref. 42. There are not enough details given in Ref. 47 to permit a more critical examination of the results. For example, the pressure distributions on the wings are not given. Nash and Bradshaw (Ref. 48) have shown

that drag of excrescences on bodies such as airfoils can be much greater than the same roughness on a flat plate. This suggests that the tripping power of roughness may also be greater on airfoils where local velocities exceed free stream.

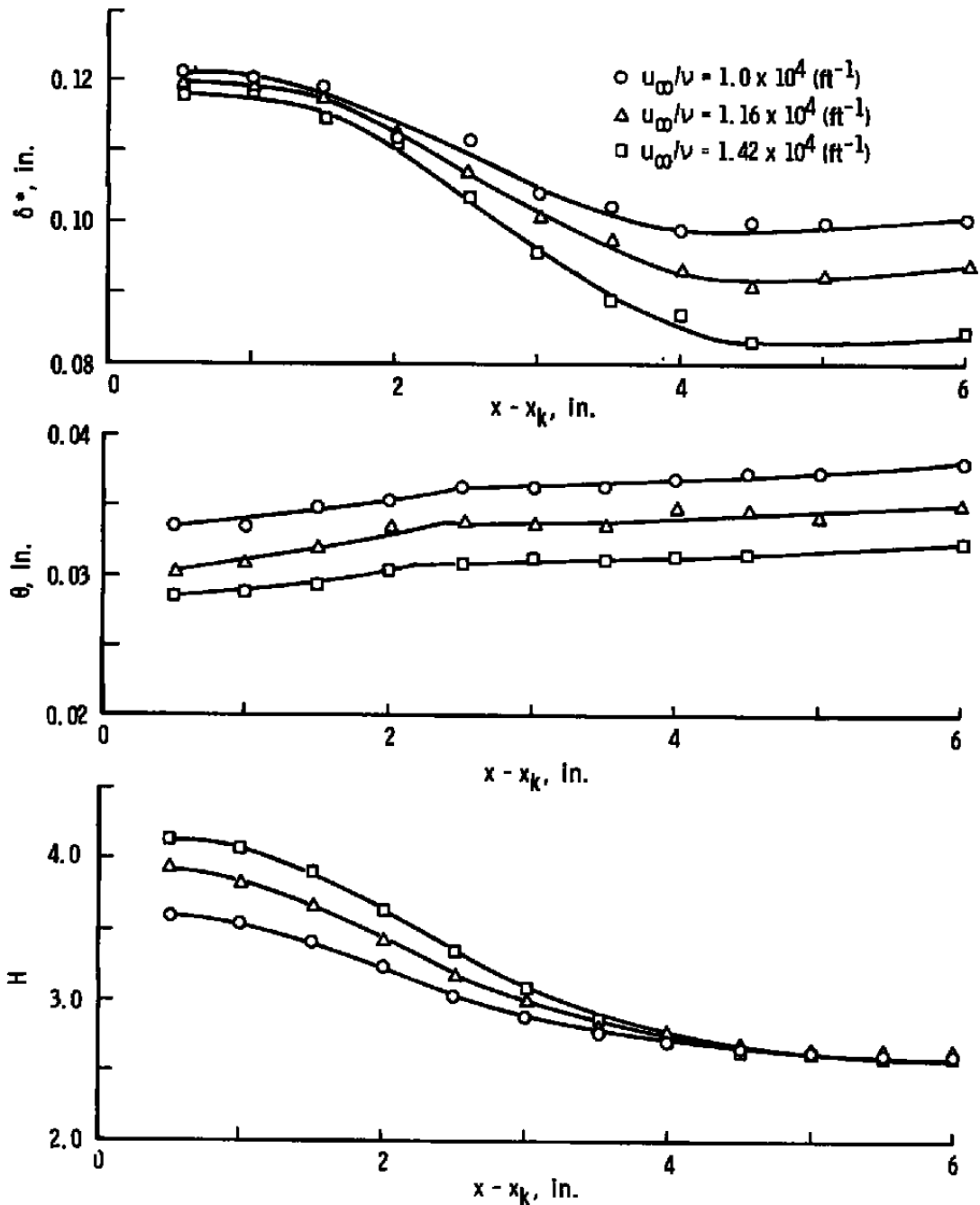


Figure 18. Distribution of boundary layer parameters downstream of 0.066-in.-diam roughness elements at $x_k = 2$ ft. From Klebanoff and Tidstrom (Ref. 35)

The Nash-Bradshaw analysis presents an insight or framework for understanding the manner in which a perturbation in boundary layer momentum thickness adds to profile drag. They considered only boundary layers that are already turbulent at the roughness element. However, if it is assumed that transition occurs in a short distance downstream of the roughness, the excrescence-drag magnification factor due to a non-flat-plate flow is applicable. To estimate excrescence drag, it is necessary to have a value for the $\Delta\theta$ added by the roughness (cf. Fig. 18).

To gain some appreciation of the relative sizes of boundary layer trips that may be necessary in a transonic flow, results of a simple example are tabulated below. Because of its convenience, plus the present concern with transition near the trips, the method of Van Driest and Blumer (Ref. 45) is followed. The calculated trip height, k , is said to correspond to the minimum transition Reynolds number. However, the k is not usually large enough to bring about transition at the trip ($x_t \approx x_k$). This distinction must be made because the decrease of x_t as k or U/ν increases usually slows as $x_t \rightarrow x_k$ and a minimum Re_t for a given k results. Therefore, it is better to view the k calculated by the method of Van Driest and Blumer or Braslow et al. as a trip height that gains the most forward movement of x_t that can be accomplished "easily," i.e., without encountering the stiffening resistance that arises when there is an effort to move x_t too near to x_k . The procedure given by Potter and Whitfield (Ref. 42) has the advantages of predicting the movement of x_t for any $x_k < x_t < x_{t0}$, up to the case $x_t \approx x_k$, and the use of the untripped transition station, x_{t0} , in the correlation removes the influence of "wind-tunnel-peculiar" conditions which affect transition. However, a more tedious computation is necessary when $k < \delta_k$, and the value of Reynolds number of transition without roughness is required.

Because the method of Ref. 42 attempts to encompass the case $x_t \approx x_k$, it often has been used to determine a value of k for that case, when the user of the method would have had better results by only taking k large enough to bring about the decrease of x_t to the "near x_k " station such as the "effective x_t " of Ref. 45. This would follow from limiting the tripping parameter to $Re_k/\epsilon = 0.8 - 0.85$ rather than 1.0 in the method of Ref. 42.

To furnish an example of the sizes of trips that may be required in a transonic wind tunnel case, the simpler, though less general, method of Ref. 45 is applied to representative (hypothetical), 2-D, flat-plate flow conditions specified in Table 2. The results given there are presented as a ready reference to the range of k/δ_k encountered under typical transonic wind tunnel conditions.

There are circumstances which will alter the required sizes of trips or their effectiveness. Among those is the local flow field such as already mentioned in regard to the effect of pressure gradients. In addition, it should be noted that Ref. 42 shows that when $M_k < 1$, a

2-D roughness element is more effective than the 3-D grit roughness for which Ref. 45 and Table 2. apply. This enables a much lower k/δ_k in subsonic flow if a 2-D element meets other requirements. Secondly, sweep apparently decreases transition Reynolds numbers as demonstrated, e.g., by Jillic and Hopkins (Ref. 49). They found that free-stream Reynolds number of transition was decreased more than could be accounted for by the shock loss at a blunt leading edge. Their data for $M_\infty = 0.27$, where no leading-edge shock could exist, are shown in Fig. 19. Figure 20 shows the effect of sweep when combined with the effect of leading-edge bluntness and normal shock formation at $M_\infty = 2$. Greater reductions in Reynolds number were found in the case of supersonic flows, where leading-edge shock loss is decreased as sweep increases. (The dashed curve in Fig. 20 represents the computed effect of a normal shock wave on local Reynolds numbers.) This situation will make for easier boundary layer tripping; i.e., less trip height will suffice on swept wings. The marked drop in Reynolds number ratio and occurrence of separation when the leading-edge flow component became subsonic in Fig. 20 should be noted.

Table 2. Example Trip-Size Estimates (Method of Ref. 45)

Assumed Conditions, $M_e = 1.00$, $(U/\nu)_e = 100,000/\text{cm}$, $T_w = T_{aw}$, 3-D Roughness Elements				
x_k cm	Re_{ek}	k , cm	k/δ_k	x_t , cm (Predicted)
1	920	0.009	0.44	1.9
2	1100	0.011	0.37	2.9
4	1300	0.013	0.31	4.9
8	1550	0.016	0.27	8.9
16	1840	0.018	0.22	16.9

The possibility of tripping in many cases without exceeding, say, $k/\delta_k \approx 1/2$ suggests that excessive boundary layer thickening attributable to trips should not be as severe a problem as widely assumed, provided one is concerned with stations where $x \gg k$. Of course, without more data such as those in Table 1, it may be wrong to conclude that $k/\delta_k \approx 1/2$ is a safe limit even when $x \gg k$. Mach number, pressure gradient, type of trip, lateral spacing of trip elements, and existence or nonexistence of spanwise flow may affect the distortion of the boundary layer downstream of the trip and the incremental drag due to the trip. That part of the added drag caused by the trip rather than the tripping, i.e., excrescence drag, has been measured by various investigators. Braslow (Ref. 43) and Winter and Gaudet (Ref. 50) have reported such data. The latter also gave an analysis and method of predicting excrescence drag. Braslow reported cases where $k = \delta_k$ did not cause added drag, δ_k being laminar boundary layer thickness. However, that is not a general criterion. Trip-added drag apparently is magnified when local velocities exceed free-stream values, cf. Nash and Bradshaw (Ref. 48).

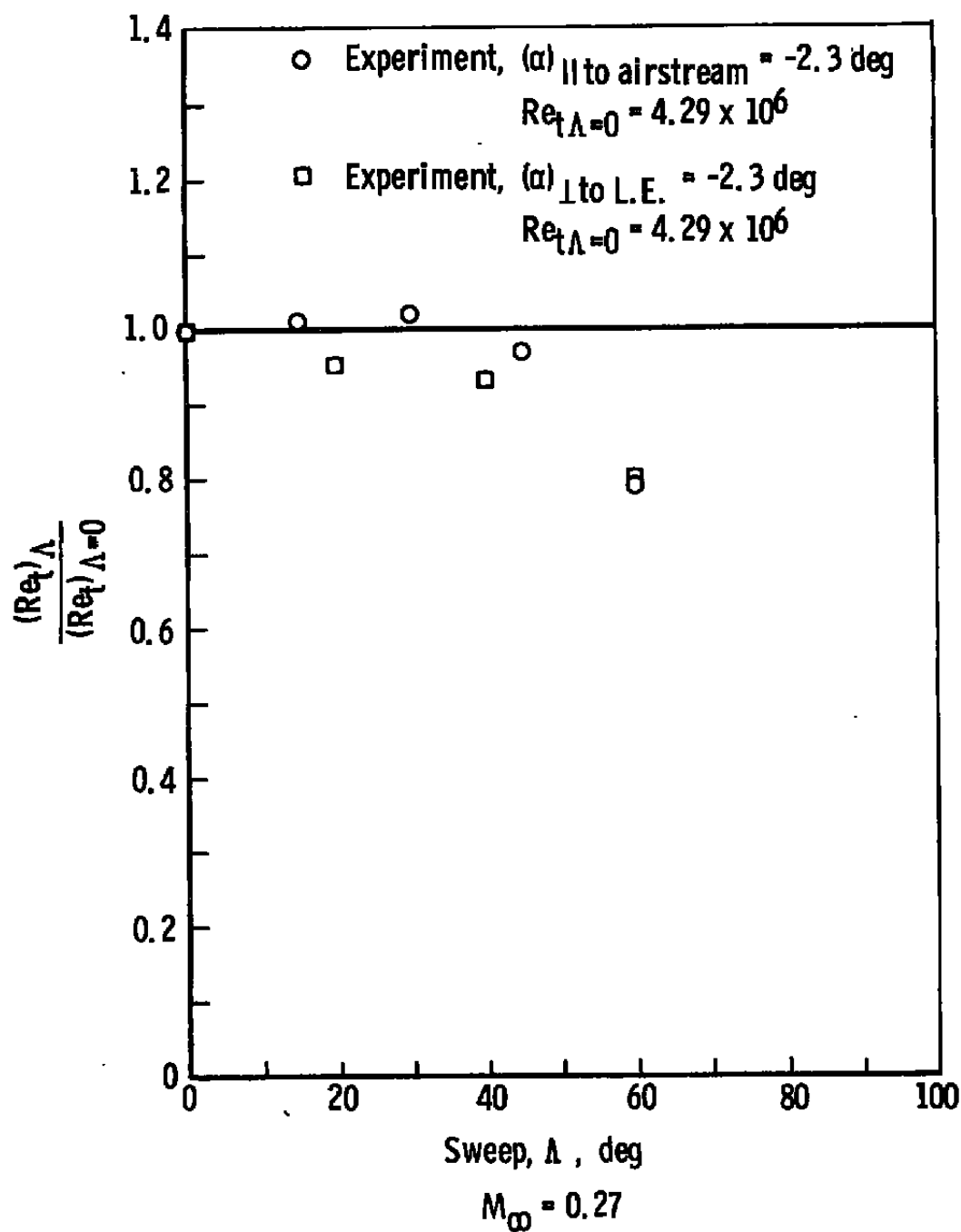


Figure 19. Variation of the normalized free-stream transition Reynolds number with sweep at subsonic Mach number. From Jillie and Hopkins (Ref. 49)

There is another aspect of the boundary layer problem that arises even when the trip adds little to the thickness. A low Reynolds number boundary layer that is laminar over a distance

of approximately x_k and turbulent thereafter can equal the relative thickness (δ/c) of a high Reynolds number layer that is naturally turbulent from $x_t \approx 0$ only under certain conditions. Matching of relative thicknesses, δ^*/c , θ/c , at equal values of $(x/c)_s$, shock location, between a wind tunnel case and a higher-Reynolds-number flight case depends on the satisfaction of several flow and geometric relations which is not always feasible.

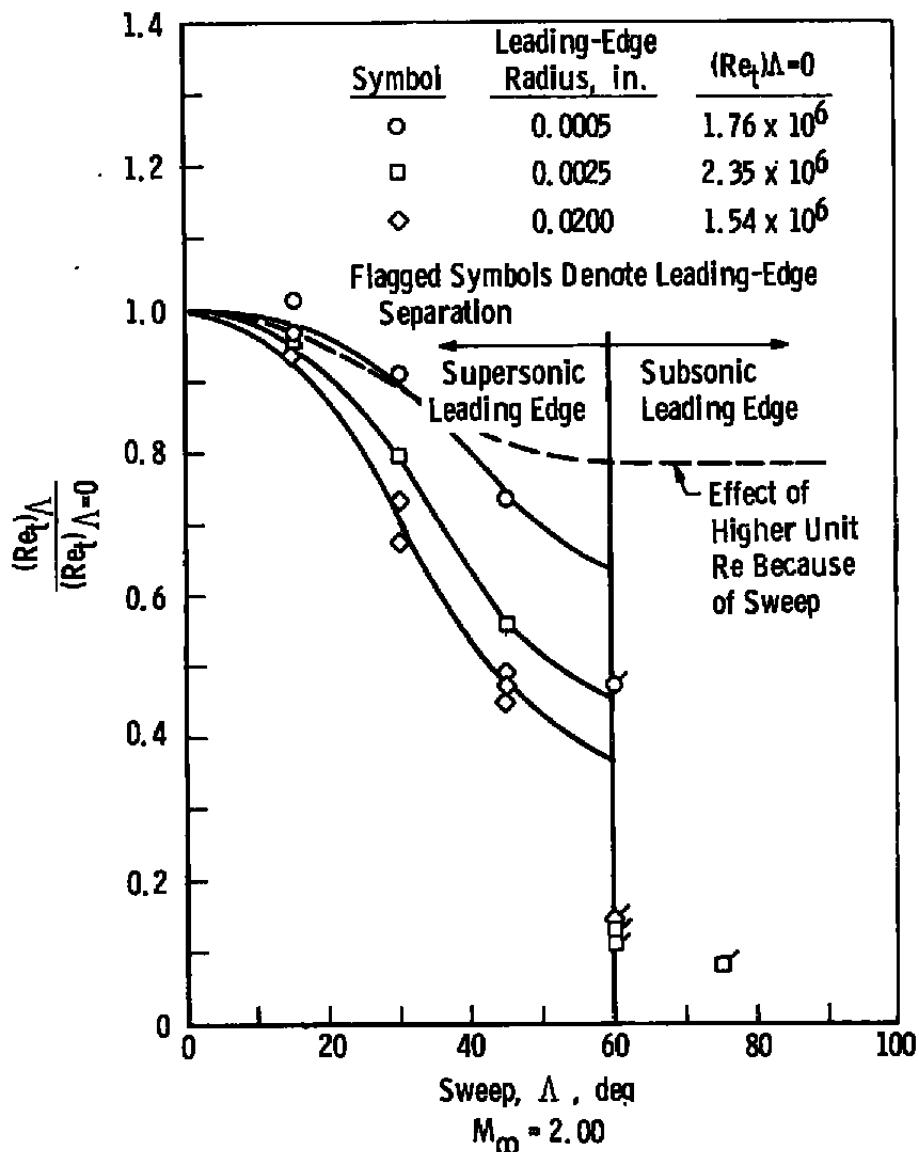


Figure 20. Variation of the normalized free-stream transition Reynolds number with sweep at supersonic Mach number. From Jillic and Hopkins (Ref. 49)

The trade-off of the effects of local Mach number and local Reynolds number at the boundary layer edge should be kept in mind when choosing trip location. The rapid increase in boundary layer stability through the transonic Mach number range causes a corresponding rate of increase in trip sizes if unit Reynolds number is not also increasing enough to compensate for the Mach number effect, cf. Ref. 42.

4.2 VORTEX GENERATORS

The use of vortex generators to inhibit boundary layer separation is an established practice. Figure 21, from Cahill (Ref. 51), is an interesting example. With transition fixed at $x_t/c = 0.10$ and $\alpha \approx 0$ deg, shock location and trailing-edge pressure at $Re_c = 2.8 \times 10^6$ were nearly the same as found for $Re_c = 8.5 \times 10^6$ if vortex generators were located upstream of the shock (diamond symbols in Fig. 21). When the shock moved ahead of the vortex generators, at $\alpha = 1$ to 2 deg, the trailing-edge pressure and shock location dramatically shifted to the levels corresponding to lower Reynolds numbers. That underscores the problem with either trips or vortex generators at fixed locations. Transition, shock waves, and separation move about as Mach number and/or angle-of-attack change. Thus, no single trip or vortex generator position is likely to satisfy all test requirements. This problem was encountered long ago, and for the trips, some degree of flexibility sometimes has been gained by doing the tripping with gas jets that could be varied in strength. Additional flexibility also may be achieved by arranging to exhaust the jets at varying stream-wise locations, but that obviously requires a more complex model.

Under some circumstances, it may be feasible to combine the vortex generation and trip function, i.e., use the generators as trips. Some trade-off in effectiveness in fulfilling each function can be expected. For example, the higher velocities near the surface in a turbulent boundary layer probably enhance vortex generator performance, but the thicker turbulent boundary layer may offset that advantage.

The design of vortex generators has been discussed by Powers (Ref. 52) who has given criteria for generator angle of attack, spacing, aspect ratio, and height. The function of vortex generators is to cause the transport of higher speed air from the outer part of a boundary layer into the lower speed region nearer to the solid surface. When adjacent generators are canted so that counter-rotating vortices are formed, the boundary layer flowing between the pair can be made much thinner. This suggests that vortex generators may be used to simulate a boundary layer at a higher Reynolds number if the added drag of the generators is acceptable. Considering that a generator need be no higher than δ , will be at an incidence of approximately 16 deg with the local flow, will have an aspect ratio near 1,

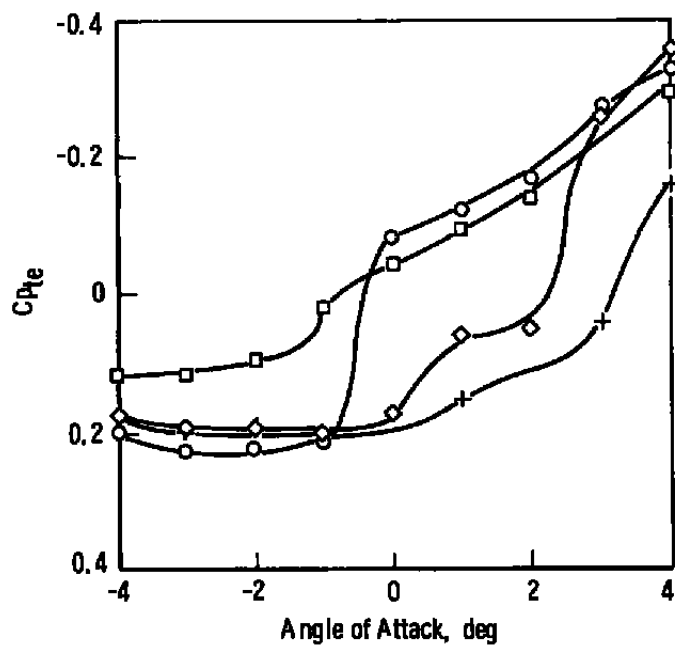
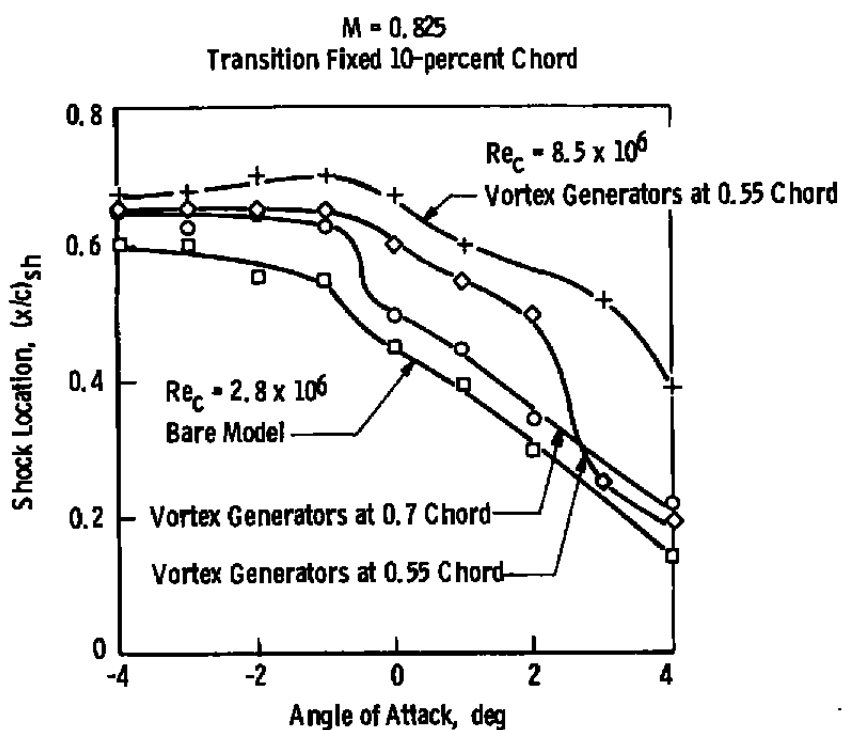


Figure 21. Effect of vortex generators on shock location and pressure recovery. From Cahill (Ref. 51)

and be spaced about 3.5 generator heights from its neighbors, it would seem that the extra "trip" drag would be no worse than that caused by rows of grit or other conventional trips. Unfortunately, there seems to be no data on the development of transition downstream of vortex generators, so their performance as trips cannot be compared to the usual 2- or 3-D trips. Aside from the added work in making such devices, another disadvantage is the spanwise nonuniformity because of the wake-like flow that will exist upstream of the station where merging occurs.

4.3 FREE-STREAM TURBULENCE

Not only is free-stream turbulence a factor in determining boundary layer-transition Reynolds number, it is also known to affect boundary layer thickness and detailed characteristics within the layer. Raghunathan and McAdam (Ref. 53) have presented data for turbulent boundary layer flow over a half-biconvex airfoil mounted on the wall of a transonic wind tunnel. Ratios of total and momentum thicknesses and shape factors across the shock are given. Increasing free-stream turbulence causes δ_2/δ_1 and H_2/H_1 to decrease, while θ_2/θ_1 increases rather slowly. Separated flow region at the trailing edge was decreased as free-stream turbulence increased. In Ref. 54 the same authors presented data for the same experimental arrangement which show shock position shifted downstream as free-stream turbulence was increased.

Green (Ref. 55) reviewed earlier data on flat-plate flows that predicted that increased stream turbulence (at constant Re_θ) will alter skin-friction coefficients and shape factors according to the relations, $\Delta c_f/c_f = 4.8 u'/u_e$, and $\Delta H/H = -(2.4 - 0.25H)u'/u_e$. Green concluded that the "effective" Reynolds number increases rapidly with u'/u_e and that the sensitivity is greater at higher Reynolds number. In a typical example, for an airfoil, he found that a 1-percent increase of turbulence could have the same effect as increasing the Reynolds number by 60 to 70 percent.

These findings, not surprisingly, have inspired some to suggest that elevating free-stream turbulence is a way to gain the effects of higher Reynolds number. However, Green cautioned that there were unanswered questions about the validity of that technique. He pointed out that the role of turbulence scale as well as intensity would have to be investigated; the response of the boundary layer on the model may vary depending on its scale; and acoustic disturbances may not affect a boundary layer in the same way as vortical disturbances coming from upstream. Other objectional features of this technique that can be foreseen are the need to calibrate the turbulence and its equivalent Reynolds number and the detailed relationship between turbulence and its influence on model measurements even when transition is not a factor (cf. Durbin and Hunt, Ref. 56).

In particular, the possibility that intensity and scale of turbulence may each affect boundary layer flow in an interrelated fashion cannot be ruled out. This would make any effort to control "effective" Reynolds number by manipulating stream turbulence very risky. It opens another subject of research. Of course, one cannot say that turbulence scale effects are not involved in conventional boundary layer tripping either. Scale of trip-produced turbulence probably is related to trip size, local Reynolds number, and distance downstream of the trip. It is possible that scale effect, if it is significant, may be accounted for by the usual practice of evaluating trip effectiveness in terms of a trip height-Reynolds number parameter.

5.0 WIND TUNNEL TESTING PRACTICES

A report which was written by Haines et al. (Ref. 57) over twenty-six years ago presents a rather thorough discussion of various problems encountered in fixing transition on wings in transonic wind tunnel tests. Most of the noted difficulties remain to this day. A few of the more recent reports in the same area are Refs. 11, 58, and 59. The latter also covers other transonic wind tunnel testing problems. A general impression left by all such discussions is that extra effort in collecting data and thoughtfulness in analysis are essential if the best results are to be achieved in subscale wind tunnel testing. Routine methods, inflexible test plans, and minimal tunnel occupancy time often will lead to later surprises when full-scale data become available.

Tripping of the boundary layer is not necessarily sufficient to assure simulation of higher Reynolds numbers, the problem can be much more complex. Different unit Reynolds numbers, different scales (model sizes), different trip sizes and locations, judicious use of vortex generators, guidance by computed results, measurement of boundary layer characteristics at key locations, and thoughtful study of results will, in general, all be required in order to minimize the error when the test results are extrapolated to full-scale conditions. The greater uncertainty generally will be associated with 3-D flows and flows including significant shock wave-vortex-transition and separation interactions.

If wind tunnel testing is to be done at less than full-scale Reynolds number, it should be guided by results of analytical efforts that provide estimates of full-scale boundary layer and shock wave characteristics. Otherwise, the testing is done without knowing approximately the conditions that will indicate how well full-scale Reynolds numbers are simulated. The experimentation will include determination of boundary layer-transition location on a smooth model, possibly using a subliming film for visual location of transition at various free-stream unit Reynolds numbers. It must be remembered that boundary layer-transition Reynolds number usually varies with unit Reynolds number, and other properties of the test-section flow of transonic wind tunnels also often vary with unit Reynolds number. Thus,

Reynolds number effects appearing in model measurements must not be confused with those caused by free-stream flow changes accompanying changes of unit Reynolds number.

Pressure distribution, or at least trailing-edge pressure, and boundary layer thicknesses at the trailing edge or ahead of the shock may also be measured and used as a criterion for scaling viscous effects. Then, it is usual for roughness to be fixed so as to cause transition at location(s) simulating full-scale boundary layer conditions at the critical location on the body. Pressures are again measured to determine if the expected full-scale shock position has been achieved.

There are two approaches to tripping, which may be classified as "forward tripping" and "aft tripping." The first and perhaps more traditional forward tripping involves tripping at the percent of chord where transition is predicted under full-scale conditions; then measurements made at each of a series of Reynolds numbers are extrapolated to predict the full-scale results. Aft tripping is done in order to minimize δ^*/c at the shock while still assuring a turbulent boundary layer there. That approach seems to have more followers, but it cannot always be used. When conditions are such that the shock or separation are far forward, tripping, to be effective, must occur still farther forward, and the distinction between forward and aft tripping may vanish. One may list advantages and disadvantages for both approaches, and neither will necessarily assure that trailing-edge boundary layer conditions, which affect lift and drag, are closely simulated. Some experimenters will choose to use each method, depending on the particular quantity being measured. Any measurements that involve significant fore and aft movement of separation or shock obviously are going to cause problems with aft tripping. There may be conditions for which "no tripping" is the preferred approach. Unfortunately, it may be impossible to forecast what technique is best, and a test plan should allow for alternatives.

If there is concern over excrescence drag, the drag of the model with varying trip heights and locations may be measured. If possible, schlieren or shadow photography may be used to supplement other data. Vortex generators also may be used to delay separation and simulate higher Reynolds number conditions on the model. All of these data have to be collected at each angle of attack. The pressure distributions may be used in the method of Ref. 15 to estimate shock position and pressure distribution at flight Reynolds numbers. If full pressure distributions are not taken, the trailing-edge pressure provides the indication of which trip and/or vortex generator configuration has achieved the highest effective Reynolds number.

It is apparent that estimates of full-scale boundary layer thickness and transition location will be needed if the effective wind tunnel Reynolds numbers are to be estimated. That is, the tripped boundary layer with its corresponding characteristics and transition location has to

be related to an untripped, higher Reynolds number condition. Transition location alone could be used as the scaling criterion, but that usually is inadequate. More detailed knowledge of the tripped layer is needed because thicknesses and shape factors offer a way to judge if separation is also properly scaled.

If vortices and vortex-shock interaction are features of the flow, it will be necessary to try to assure that the line of separation is the same on the model as it would be at flight Reynolds numbers. This may require that leading-edge roughness be used, and the minimization of boundary layer thickening due to the tripping is critical. Various computational estimates of separation location may be used to assess Reynolds number effects. The interaction of vortices with adjacent surfaces will make it important to achieve the same vortex pattern as will exist in flight (Ref. 59). In all transonic testing the criticality of Mach number as a parameter cannot be overemphasized. That is also a troublesome factor when attempting to compare flight and wind tunnel data because a close match in Mach numbers is required when near Mach one.

It is important that the type(s) of separation be identified in the early phase of testing so that the essential requirements for simulation are known. This information is also needed as a check on the applicability of Ref. 15 if that procedure is to be used.

5.1 SCALING FOR AERODYNAMIC COEFFICIENTS

No attempt is made to discuss all possible scaling procedures, but the simpler procedure appropriate for airfoils or wings at low angles of attack is briefly considered as an example. We concentrate on a few of the aerodynamic qualities that have to be scaled when transonic test data are obtained in wind tunnels that do not match free-flight Reynolds numbers. Foremost of these is shock location on wings which has been discussed earlier and will not be reviewed again. However, the attainment of the full-scale shock location is the underlying basis of what follows.

Drag coefficient is one of the first aerodynamic coefficients thought of in the context of Reynolds number deficiency. The common approach is to acquire data over the available Reynolds number range and then extrapolate the friction-drag component or the total drag coefficient to the desired Reynolds number according to an appropriate friction-drag law. "Form factors" are used as corrections to flat-plate friction drag to account for the shape of the airframe components. For this procedure to be valid, the location of boundary layer transition must either be fixed or its variation with Reynolds number known, and no further significant change in shock wave or separation locations can occur. Potential errors in this procedure are easy to identify, but it is a widely used technique, and the only avenue toward

improvement would seem to be work on details of the basic method. For example, newer CFD capabilities will improve the predicted friction-drag variation. In time, CFD will enable the entire viscous flow field, including separation to be scaled more precisely on a routine basis.

The relatively straightforward approach to correcting drag coefficients should not lead to undue optimism about extrapolation procedures in general. It is possible for movements of transition and/or separation to cause trouble. A sobering example is presented by Stanewsky (Ref. 60). His data show a reversal of trends of lift coefficient at drag-rise Mach number, as well as variation in that Mach number, in the neighborhood of $Re_c = 10^7$ when free transition is allowed. With transition fixed well forward, neither C_L nor M_∞ at drag rise agreed with those values or even their trends for free transition at the maximum Reynolds number of 3×10^7 .

It has to be remembered that there are mutual interactions between boundary layer characteristics, shock locations, and separations, and these are varying as unit Reynolds and Mach numbers and angle-of-attack changes. Thus, there can be unexpected results that do not follow simple extrapolations of lower Reynolds number data. One must keep their attention on the more significant parameters that influence the viscous-inviscid interactions if these results are to be anticipated. For example, if one wants to know what will happen if unit Reynolds number is increased, they have to be mindful of the effects on transition location and boundary layer characteristics, the influence of these factors upon separation development and shock location, and finally the net effect upon pressure distribution. The interdependence of all of these will often make accurate extrapolations or scaling impossible, particularly when 3-D flow is involved.

Stanewsky's (Ref. 60) research has shown that supercritical airfoils are very sensitive to viscous effects. He has demonstrated that changes in unit Reynolds number produced different lift coefficients even at low α , and that reversals in movement of transition location occurred as angle of attack changed because of accompanying variations of boundary layer thickness and effective airfoil shape. Stanewsky's transonic sensitivity parameter for airfoils at given M_∞ and Re_c was shown in Ref. 60 to correlate the ratio of change in C_L to change in transition location on a number of airfoils.

One approach for attempting to determine aerodynamic coefficients for an airfoil or wing at low angle of attack for free-flight Reynolds number may be based on the attainment of full-scale shock position in the subscale, low Reynolds number tunnel test. See earlier discussion and Fig. 22 for the justification of this approach. It follows from conditions (1) through (4) in Section 3.0. The following steps would be involved, for given M_∞ and α :

1. Estimate transition location, $(x/c)_t$, for no trips and then determine trip sizes to bring about transition at a series of lesser $(x/c)_t$. The intent is to bring about a turbulent boundary layer of the least feasible thickness ahead of the shock.
2. Measure C_L , C_D , C_M , $(x/c)_{sh}$ and C_{pte} at each $(x/c)_t$ at the maximum chord Reynolds number.
3. Plot the measured data as in Fig. 23. If the rearmost relative shock position, $(x/c)_{sh}$ is the same as will exist at full-scale, the coefficients corresponding to that shock position should be approximately the ones for full-scale Reynolds numbers.
4. Using measured C_{pte} , apply the method of Ref. 15 to further check on shock position. (The limitation on that method relative to bubble separations has to be observed.) Data at various spanwise stations for a wing model and for other Reynolds numbers may also be needed.
5. If pressure recovery over the aft part of the chord is less than expected, vortex generators may be tested at several chordwise positions upstream of the shock to learn if shock position is moved farther aft (see Fig. 21 in this regard).
6. If vortices are a feature of the flow, the foregoing procedure should be carried out both for vortices burst (broken down) and unburst. Tripping may not be feasible (see earlier discussion), but an effort has to be made to at least bracket the low and high Reynolds number vortex conditions (see Fig. 15).

It cannot be guaranteed that this procedure will automatically lead to the correct full-scale aerodynamic coefficients, and it will not always be possible to approach closely enough to conditions (1) through (4) of Section 3.0. Also to be noted is the need for more information than merely the low Reynolds number wind tunnel data to carry out this procedure. The experimental data have to be supplemented by CFD and correlations such as provided in Ref. 15.

If there is uncertainty about transition location and no preliminary experiment for the purpose of locating transition is conducted, the "eⁿ" method may be used. A recent report by Wazzan et al. (Ref. 62) and other references therein may be referred to for this computation. However, it would be well for users of the "eⁿ" method to read the paper by Mack (Ref. 63). Because of the strong destabilizing influences present in transonic wind tunnels, empirical data from the particular tunnel to be used probably will be relied on by many experimenters. Comparative data from many tunnels have been reported by Dougherty and Steinle (Ref. 64) and Dougherty and Fisher (Ref. 65). A recent paper by Harvey (Ref. 66) reviews transonic tunnel and flight transition results in relation to free-stream disturbances.

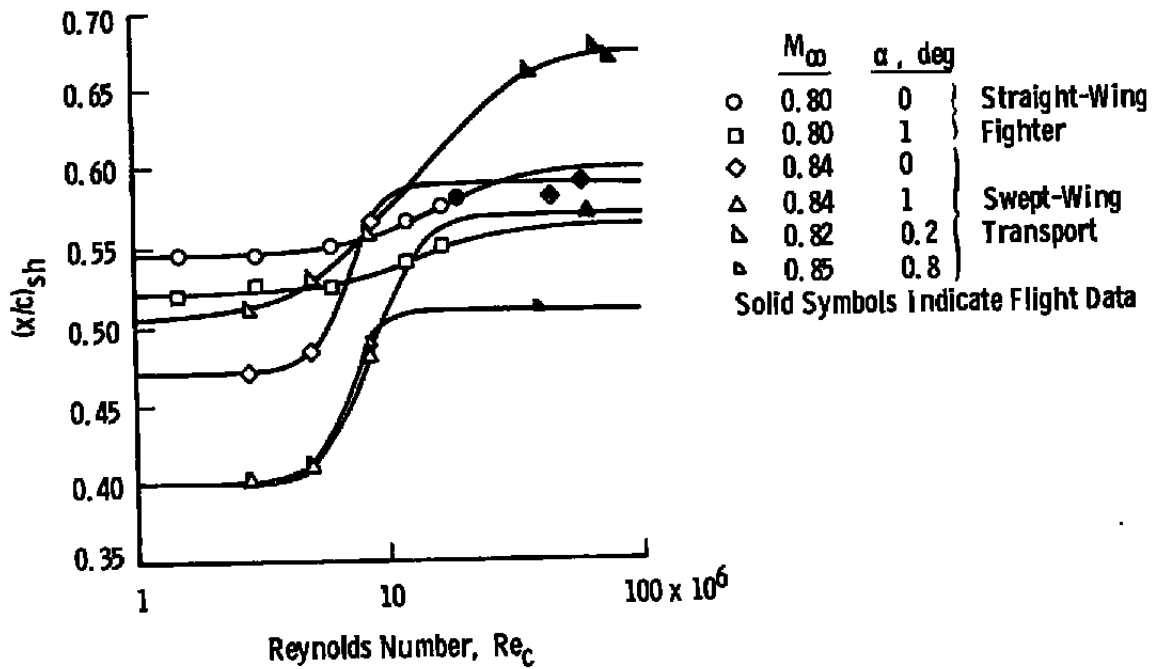


Figure 22. Variation of shock location with Reynolds number.
From Baals (Ref. 61)

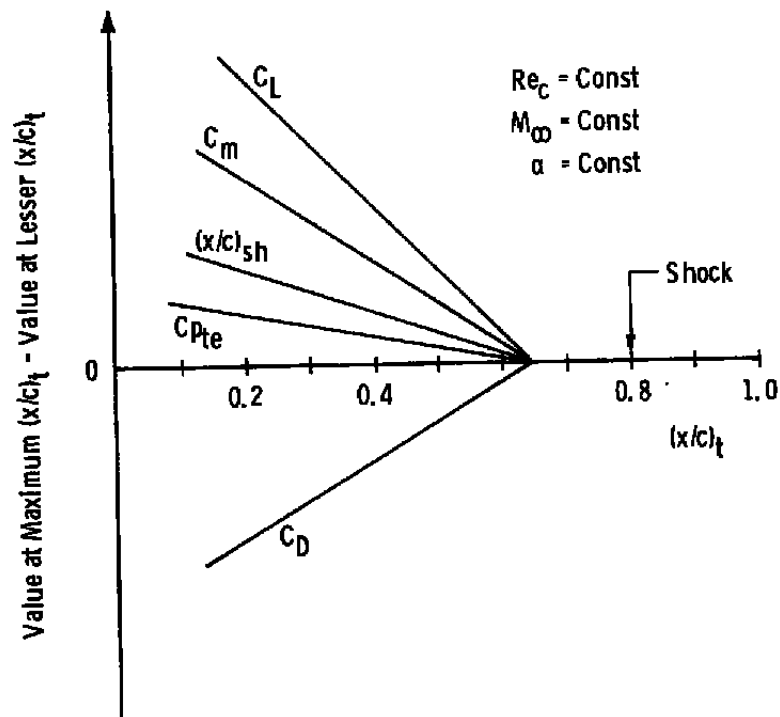


Figure 23. Idealized graphical trend of data with transition location.

6.0 CONCLUDING REMARKS

When this subject was discussed over ten years ago, all of the parts of the problem were recognized. However, there is now a clearer understanding of several features of transonic, viscous-flow simulation. While these improvements should lead to better degrees of simulation, they do not make the experimenter's task easier. For example, it has been shown that when unit Reynolds number and wetted length are varied separately, different effects on separation pressure coefficient are produced (Ref. 12). This type of effect also has been demonstrated in the upstream influence of 2- and 3-D compression corners (Ref. 13). Thus, the experimenter cannot be satisfied with merely matching Reynolds numbers when investigating shock wave-boundary layer interactions.

Melnik's viscous, transonic simulation parameter, K_t , shows that Reynolds number (or c_f) affects upstream influence of shocks even though the boundary layer is turbulent. This imposes an extra burden on scale-model testing; i.e., simply achieving a turbulent boundary layer ahead of the shock is not sufficient for simulation of high Reynolds numbers.

Another aspect of the simulation problem on which more light has been shed is the Reynolds number effect on separated and vortical flows. It has been shown that changes in aerodynamic loads because of vortices may persist at very large Reynolds numbers (Ref. 22), and use of boundary layer trips may so influence vortex formation that simulation would be entirely lost (see Fig. 16). This serves as a clear warning of the danger of assuming that all vortical flows are immune to Reynolds number effects. Shock interaction and vortex bursting may be influenced by large changes in Reynolds number, and the possibility of relatively large changes in aerodynamic coefficients should not be ignored.

Data on the new supercritical airfoils reveal strong sensitivity to viscous effects. Stanewsky (Ref. 60) has convincingly documented this.

The experimenter is compelled to recognize several general features of viscous, transonic-flow simulation, viz.,

- The technique must be tailored to the vehicle configuration, local flow characteristics, and the type of aerodynamic data sought.
- Tripping the boundary layer at forward stations does not, in general, assure adequate simulation of higher Reynolds numbers.
- Procedures that may be referred to as "no boundary layer tripping," "aft tripping," and "forward tripping" may each have its place in a test program. Tripping can sometimes conceal Reynolds number effects.

- Other free-stream flow properties of transonic wind tunnels often vary with changes in free-stream unit Reynolds number, thereby creating confusion between "real" and "spurious" viscous-flow effects.
- Any procedure will have to offer guidance and alternatives; it cannot be followed blindly without incurring risk.

A rational subdivision of aerospace vehicles or components and some characterizations follow:

1. Transport wings — low angles of attack; higher Reynolds numbers; most extensively studied; great accuracy required in predicting coefficients.
2. Delta wings — vortical flows even at relatively low angles of attack; may be difficult to simulate high Reynolds numbers because of flow developments very near leading edges.
3. Missile and aircraft forebodies — high angles of attack; vortical flows; difficult to predict results; sometimes large effects of Reynolds number.
4. "Complex" configurations — a category of complicated flows possibly involving canards; leading-edge flaps; relatively large inlet and nozzle-afterbody influences; external stores, vectored nozzles, etc.

Regarding category (1) above, the current questions concern whether forward tripping and extension of wind tunnel data to predict full-scale aerodynamic coefficients by simple trend extrapolation with Reynolds number is superior to aft tripping with an effort to simulate essentially full-scale flow conditions at tunnel Reynolds number. There is also concern over whether matching of boundary layer properties just ahead of the terminal shock or at the trailing edge is best. Actually, all of these have their places, but it is often unclear which plan is best without trying all of them.

For category (2), it will sometimes only be possible to bracket the low and high Reynolds number aerodynamic coefficients. A particular problem arises because the physical space available for manipulating the boundary layer may be of the order of 10 percent of the chord, or less, at the leading edge. In the case of category (3), tripping can be ineffective or misleading. The many different and complex interactions possible in category (4) make a fixed procedure elusive. None is suggested herein.

These are only some of the complexities of transonic, viscous-flow simulation and scaling that have been brought out in recent years. The National Transonic Facility (NTF) at Langley Research Center is going to offer much greater Reynolds numbers in a ground test

facility, so that an increased rate of learning may be anticipated. However, much testing will continue to be done in the older, conventional tunnels now in use. This review stresses the need for more extensive, systematic experimental procedures, backed up by CFD and painstaking analysis, if the quality of information derived from low Reynolds number tests is to be improved.

REFERENCES

1. Chang, Paul K. *Control of Flow Separation*, Hemisphere Publishing Corp., Washington, D.C., 1976, p. 213.
2. Pearcey, H. H., Osborne, J., and Haines, A. B. "The Interaction Between Local Effects at the Shock and Rear Separation — A Source of Significant Scale Effects in Wind-Tunnel Tests on Airfoils and Wings." *Transonic Aerodynamics*, AGARD CP 35, September 1968.
3. Osborne, J. and Pearcey, H. H. "A Type of Stall with Leading-Edge Transonic Flow and Rear Separation." *Facilities and Techniques for Aerodynamic Testing at Transonic Speeds and High Reynolds Number*, AGARD CP 83, August 1971.
4. Yoshihara, H. and Zonars, D. "The Many Facets of 3D Transonic Shock Induced Separation." AGARD CP 168, November 1975.
5. Green, J. E. "Interactions Between Shock Waves and Turbulent Boundary Layers." *Progress in Aerospace Sciences*, Vol. 11, D. Kuchemann, ed., Pergamon Press, Oxford, 1970.
6. Reshotko, E. and Tucker, M. "Effect of a Discontinuity on Turbulent Boundary Layer Thickness Parameters With Application to Shock Induced Separation." NACA TN 3454, May 1955.
7. Green, J. E. "Some Aspects of Viscous-Inviscid Interactions at Transonic Speeds, and Their Dependence on Reynolds Number." *Facilities and Techniques for Aerodynamic Testing at Transonic Speeds and High Reynolds Number*, AGARD CP 83, August 1971.
8. Settles, G. S., Bogdonoff, S. M., and Vas, Q. E. "Incipient Separation of a Supersonic Turbulent Boundary Layer at High Reynolds Numbers." *AIAA Journal*, Vol. 14, No. 1, January 1976, pp. 50-56.

9. Melnik, R. E. "Turbulent Interactions on Airfoils at Transonic Speeds—Recent Developments." *Computation of Viscous-Inviscid Interactions*, AGARD CP 291, February 1981.
10. Hall, M. G. "Scale Effects in Flows Over Swept Wings." *Facilities and Techniques for Aerodynamic Testing at Transonic Speeds and High Reynolds Number*, AGARD CP 83, August 1971.
11. Haines, A. B. "Possibilities for Scale Effect on Swept Wings at High Subsonic Speeds." *Facilities and Techniques for Aerodynamic Testing at Transonic Speeds and High Reynolds Number*, AGARD CP 83, August 1971.
12. Stanewsky, E. and Little, B. H., Jr. "Separation and Reattachment in Transonic Airfoil Flow." *Journal of Aircraft*, Vol. 8, No. 12, December 1971, pp. 952-958.
13. Settles, G. S., Perkins, J. J., and Bodgonoff, S. M. "Upstream Influence Scaling of 2D and 3D Shock/Turbulent Boundary Layer Interactions at Compression Corners." AIAA Paper No. 81-0334, January 1981.

See also Settles, G. S. "Compressible Turbulent Boundary Layer Interaction Experiments." NASA CR 164292, May 1981.
14. Cahill, J. F. and Connor, P. C. "Correlation of Data Relating to Shock-Induced Trailing Edge Separation and Extrapolation to Flight Reynolds Number." NASA CR 3178, September 1979.
15. Khan, Mohammad M. S. and Cahill, Jones F. "New Considerations on Scale Extrapolation of Wing Pressure Distributions Affected by Transonic Shock-Induced Separation." Lockheed Georgia Company LG 83ER0055, March 1983.
16. Moss, G. F. "Some UK Research Studies of the Use of Wing-Body Strakes on Combat Aircraft Configurations at High Angles of Attack." *High Angle of Attack Aerodynamics*, AGARD CP 247, January 1979.
17. Rogers, E. W. E. and Hall, I. M. "An Introduction to the Flow about Plane Swept-Back Wings at Transonic Speeds." *Journal of the Royal Aeronautical Society*, Vol. 64, No. 596, August 1960, pp. 449-464.
18. Squire, L. C. "Experimental Work on the Aerodynamics of Integrated Slender Wings for Supersonic Flight." *Progress in Aerospace Sciences*, Vol. 20, Pergamon Press Lt., 1981, pp. 1-96.

19. Kuchemann, D. "Types of Flow on Swept Wings." *Journal of the Royal Aeronautical Society*, Vol. 57, No. 514, November 1953, pp. 683-699.
20. Smith, J. H. B. "A Review of Separations in Steady, Three-Dimensional Flow." *Flow Separation*, AGARD CP 168, November 1975.
21. Hummel, Dietrich. "On the Vortex Formation Over a Slender Wing at Large Angles of Incidence." *High Angle of Attack Aerodynamics*, AGARD CP 247, January 1979.
22. Polhamus, Edward C. and Gloss, Blair B. "Configuration Aerodynamics." *High Reynolds Number Research*, NASA CP-2183, September 1981, pp. 217-234.
23. Miller, David S. and Wood, Richard M. "An Investigation of Wing Leading-Edge Vortices at Supersonic Speeds." AIAA Paper No. 83-1816, Applied Aerodynamics Conference, July 13-15, 1983.
24. Waggoner, E. G. "Complementary Computational-Aerodynamics Research." *'National Transonic Facility Research Symposium*, NASA Langley Research Center, Virginia, December 5, 1983.
25. Keener, Earl R. et al. "Side Forces on an Tangent Ogive Forebody With a Fineness Ratio of 3.5 at High Angles of Attack and Mach Numbers from 0.1 to 0.7." NASA TM X-3437, February 1977.
26. Jorgensen, Leland H. "Prediction of Aerodynamic Characteristics for Slender Bodies Alone and With Lifting Surfaces to High Angles of Attack." *High Angle of Attack Aerodynamics*, AGARD CP 247, January 1979.
27. Pankhurst, R. C. "Technical Evaluation Report on AGARD Specialists' Meeting on Facilities and Techniques for Aerodynamic Testing at Transonic Speeds and High Reynolds Number." AGARD AR 37-71, October 1971.
28. Firmin, W. C. P. and Cook, T. A. "Detailed Exploration of the Compressible, Viscous Flow Over Two-Dimensional Airfoils at High Reynolds Number." ICAS Paper 68-09, Vth Congress of the International Council of the Aeronautical Sciences, Munich, September 9-13, 1968.
29. Blackwell, J. A., Jr. "Preliminary Study of the Effects of Reynolds Number and Boundary-Layer Transition Location on Shock-Induced Separation." NASA TN D-5003, January 1969.

See also "Effect of Reynolds Number and Boundary-Layer Transition Location on Shock-Induced Separation." *Transonic Aerodynamics*, AGARD CP 35, September 1968.

30. Bore, Cliff L. "On the Possibility of Deducing High Reynolds Number Characteristics Using Boundary Layer Suction." *Facilities and Techniques for Aerodynamic Testing at Transonic Speeds and High Reynolds Number*, AGARD CP 83, August 1971.
31. Morkovin, M. V. "Critical Evaluation of Transition from Laminar to Turbulent Shear Layers with Emphasis on Hypersonically Traveling Bodies." Martin Marietta Corporation AFFDL-TR-68-149, March 1969.
32. Reshotko, E. "Boundary-Layer Stability and Transition." *Annual Review of Fluid Mechanics*, Vol. 8, 1976, pp. 311-349.
33. Sedney, R. "A Survey of the Effects of Small Protuberances on Boundary-Layer Flows." *AIAA Journal*, Vol. 11, No. 6, June 1973, pp. 782-792.
34. Peterson, John B., Jr. "Boundary-Layer Velocity Profiles Downstream of Three-Dimensional Transition Trips on a Flat Plate at Mach 3 and 4." NASA TN D 5523, November 1969.
35. Kelbanoff, P. S. and Tidstrom, K. D. "Mechanism by Which a Two-Dimensional Roughness Element Induces Boundary-Layer Transition." *Physics of Fluids*, Vol. 15, No. 7, July 1972, pp. 1173-1188.
36. Prandtl, L. "On Boundary Layers in Three-Dimensional Flow." British Ministry of Aircraft Production Volkenrode Reports and Transactions No. 64, 1946.
37. Struminsky, V. V. "Sideslip in a Viscous Compressible Gas." NACA TM 1276, 1951.
38. Jones, R. T. "Effects of Sweepback on Boundary Layer and Separation." NACA TN 1402, July 1947.
39. Sears, W. R. "The Boundary Layer on Yawed Cylinders." *Journal of the Aeronautical Sciences*, Vol. 15, No. 1, January 1948, pp. 49-52.
40. Altman, J. M. and Hayter, N. L. F. "A Comparison of the Turbulent Boundary-Layer Growth on an Unswept and a Swept Wing." NACA TN 2500, September 1951.

41. Ashkenas, H. and Riddell, F. R. "Investigation of the Turbulent Boundary Layer on a Yawed Flat Plate." NACA TN 3383, April 1955.
42. Potter, J. Leith and Whitfield, Jack D. "Effects of Slight Nose Bluntness and Roughness on Boundary-Layer Transition in Supersonic Flows." *Journal of Fluid Mechanics*, Vol. 12, Pt. 4, April 1962, pp. 501-535.

See also "Effects of Unit Reynolds Number, Nose Bluntness, and Roughness on Boundary Layer Transition." AEDC TR-60-5 (AD-234478), March 1960.
43. Braslow, Albert L. "Effect of Distributed Granular-Type Roughness on Boundary-Layer Transition at Supersonic Speeds With and Without Surface Cooling." NACA RML 58A17, March 1958.

See also AGARD Rept. 254, April 1960, and "Use of Grit-Type Boundary-Layer-Transition Trips on Wind-Tunnel Models." NASA TN D-3579, September 1966.
44. Braslow, Albert L. and Knox, Eugene C. "Simplified Method for Determination of Critical Height of Distributed Roughness Particles for Boundary-Layer Transition at Mach Numbers from 0 to 5." NACA TN 4363, September 1958.
45. Van Driest, E. R. and Blumer, C. B. "Boundary-Layer Transition at Supersonic Speeds: Roughness Effects with Heat Transfer." *AIAA Journal*, Vol. 6, No. 4, April 1968, pp. 603-607.

See also *Journal of the Aerospace Sciences*, Vol. 29, August 1962, pp. 909-916.
46. Lyons, W. C. and Levensteins, Z. J. "The Determination of Critical Roughness Height for Boundary Layer Transition." NOL TR 61-87, October 1962.
47. Evans, J. Y. G. "Transition Fixing Techniques and the Interpretation of Boundary Layer Conditions on Slender Wings in Supersonic Wind Tunnels." *AIAA Aerodynamic Testing Conference Proceedings*, March 1964, pp. 50-58.
48. Nash, J. F. and Bradshaw, P. "The Magnification of Roughness Drag by Pressure Gradients." *Journal of the Royal Aeronautical Society*, Vol. 71, No. 673, January 1967, pp. 44-46.
49. Jillie, Don W. and Hopkins, Edward J. "Effects of Mach Number, Leading-Edge Bluntness, and Sweep on Boundary-Layer Transition on a Flat Plate." NASA TN D-1071, September 1961.

50. Winter, K. G. and Gaudet, L. "Some Recent Work on Compressible Turbulent Boundary Layers and Excrescence Drag." *Compressible Turbulent Boundary Layers*, NASA SP-216, 1969.
51. Cahill, Jones F. "Simulation of Full-Scale Flight Aerodynamic Characteristics By Tests in Existing Transonic Wind Tunnels." *Facilities and Techniques for Aerodynamic Testing at Transonic Speeds and High Reynolds Number*, AGARD CP 83, August 1971.
52. Powers, W. E. "Application of Vortex Generators for Boundary Layer Control Through A Shock." United Aircraft Corp. Research Dept. Report R-95477-6, July 11, 1952.
53. Raghunathan, S. and McAdam, R. J. W. "Boundary-Layer and Turbulence Intensity Measurements in a Shock Wave/Boundary-Layer Interaction." *AIAA Journal*, Vol. 21, No. 9, September 1983, pp. 1349-1350.
54. Raghunathan, S. and McAdam, R. J. W. "Freestream Turbulence and Transonic Flow over a Bump Model." *AIAA Journal*, Vol. 21, No. 3, March 1983, pp. 467-469.
55. Green, J. E. "On the Influence of Free Stream Turbulence on a Turbulent Boundary Layer As It Relates to Wind Tunnel Testing at Subsonic Speeds." *Fluid Motion Problems in Wind Tunnel Design*, AGARD R-602, April 1973.
56. Durbin, P. A. and Hunt, J. C. R. "Fluctuating Surface Pressures on Bluff Structures in Turbulent Winds: Further Theory and Comparison with Experiment." *Proceedings of the 5th International Conference on Wind Engineering*, Vol. 1, Colorado State University, 1979, p. V-1.
57. Haines, A. B., Holder, D. W., and Pearcey, H. H. "Scale Effects at High Subsonic and Transonic Speeds, and Methods for Fixing Boundary-Layer Transition in Model Experiments." Aeronautical Research Council R&M 3012, September 1954.
58. Stanewsky, E. and Zimmer, H. "Development and Wind Tunnel Investigation of Three Supercritical Airfoil Profiles for Transport Aircraft." NASA TM-75840, November 1980.
59. Blackwell, James A., Jr. "Experimental Testing at Transonic Speeds." *Transonic Aerodynamics*, David Nixon, Editor, *Progress in Astronautics and Aeronautics*, Vol. 81, Martin Summerfield, Series Editor. AIAA, New York, 1982, pp. 189-238.

60. Stanewsky, Egon. "Interaction Between the Outer Inviscid Flow and the Boundary Layer on Transonic Airfoils." *Zeitschrift für Flugwissenschaften und Weltraumforschung* Vol. 7, No. 4, July-August 1983, p. 242.
61. Baals, D. D. "Discussion of Paper 5." *Facilities and Techniques for Aerodynamic Testing at Transonic Speeds and High Reynolds Numbers.* AGARD CP 83-71, April 1971.
62. Wazzan, A. R., Gazley, C., Jr., and Smith, A. M. O. "The H-R_x Method for Predicting Transition." Rand Paper P-6581, January 1981.
63. Mack, L. M. "Transition Prediction and Linear Stability Theory." *Laminar-Turbulent Transition*, AGARD CP 224, October 1977.
64. Dougherty, N. S., Jr. and Steinle, F. W., Jr. "Transition Reynolds Number Comparisons in Several Major Transonic Tunnels." AIAA Paper No. 74-627, Presented at AIAA 8th Aerodynamic Testing Conference, Bethesda, Maryland, July 8-10, 1974.
65. Dougherty, N. S., Jr. and Fisher, D. F. "Boundary Layer Transition on a 10-Deg Cone — Wind Tunnel/Flight Data Correlation." AIAA Paper No. 80-0154, Presented at AIAA 18th Aerospace Sciences Meeting, Pasadena, California, January 14-16, 1980.
66. Harvey, W. D. and Bobbitt, P. J. "Some Anomalies Between Wind Tunnel and Flight Transition Results." AIAA Paper No. 81-1225, Presented at AIAA 14th Fluid and Plasma Dynamics Conference, Palo Alto, California, June 23-25, 1981.

NOMENCLATURE

C_D	Drag coefficient
C_L	Lift coefficient
C_M	Pitching-moment coefficient
C_p	Pressure coefficient
C_{p_s}	Separation pressure coefficient
$C_{p_{te}}$	C_p at trailing edge

c	Chord length (\bar{c} = average chord)
c_f	Local skin-friction coefficient
H	Boundary layer shape factor, δ^*/θ
\bar{H}	$(1/\theta) \int_0^\delta [\rho/\rho_e](1 - u/u_e)dy$
K	Khan-Cahill parameter, Eq. (6)
K_t	Melnik's parameter Eq. (3)
k	Height of roughness element
L_m	Upstream influence distance
M	Mach number
Re	Reynolds number
U, u	Velocity
u'	Fluctuating component of stream velocity
x	Streamwise, chordwise, or longitudinal coordinate
y	Coordinate normal to surface
α	Angle of attack
γ	Ratio of specific heats (1.400 for air at standard conditions)
δ	Boundary layer total thickness
δ^*	Boundary layer displacement thickness
θ	Boundary layer momentum thickness
λ, Λ	Sweep angle

ν Kinematic viscosity

ρ Gas density

SUBSCRIPTS

1,2 Upstream and downstream of shock, respectively, or before and after tripping, respectively

c Based on chord length

e Local edge-of-boundary layer value

k At top of roughness element or at station of trip

sh At shock location

t At transition

u, l Upper and lower surfaces, respectively

x Based on distance x

δ Based on δ as characteristic length

δ^* Based on δ^*

θ Based on θ

∞ Free-stream value